Article

Cell Reports

Chaperone-Mediated Sec61 Channel Gating during ER Import of Small Precursor Proteins Overcomes Sec61 Inhibitor-Reinforced Energy Barrier

Graphical Abstract

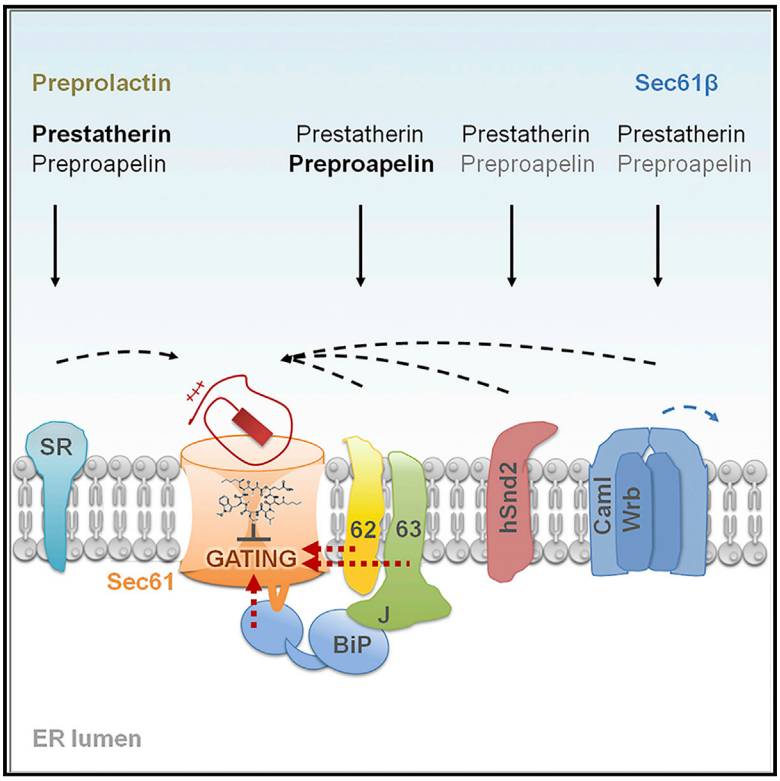

Highlights

- Small human presecretory proteins use all known targeting routes to the Sec61 complex
- Their insertion into Sec61 is selectively facilitated by BiP, Sec62, and Sec63
- Selectivity is driven by weak signal peptides plus downstream inhibitory features
- Cyclic heptadepsipeptides phenocopy the effect of BiP depletion on Sec61 gating

Authors

Sarah Haßdenteufel, Nicholas Johnson, Adrienne W. Paton, James C. Paton, Stephen High, Richard Zimmermann

Correspondence

sarah.hassdenteufel@uks.eu (S.H.), richard.zimmermann@uks.eu (R.Z.)

In Brief

Protein transport into the human endoplasmic reticulum (ER) is mediated by the heterotrimeric Sec61 channel. Haßdenteufel et al. map the determinants for requirement of different targeting pathways and different auxiliary components of the Sec61 channel in ER import of short presecretory proteins. Different characteristics of precursor polypeptides dictate the engagement of each component.

Haßdenteufel et al., 2018, Cell Reports *23*, 1373–1386
May 1, 2018
https://doi.org/10.1016/j.celrep.2018.03.122

CellPress

Cell Reports
Article

Chaperone-Mediated Sec61 Channel Gating during ER Import of Small Precursor Proteins Overcomes Sec61 Inhibitor-Reinforced Energy Barrier

Sarah Haßdenteufel,[1,*] Nicholas Johnson,[2] Adrienne W. Paton,[3] James C. Paton,[3] Stephen High,[2] and Richard Zimmermann[1,4,*]
[1]Medical Biochemistry and Molecular Biology, Saarland University, 66421 Homburg, Germany
[2]Faculty of Biology, Medicine and Health, University of Manchester, Manchester M13 9PT, UK
[3]Research Centre for Infectious Disease, University of Adelaide, Adelaide, SA 5005, Australia
[4]Lead Contact
*Correspondence: sarah.hassdenteufel@uks.eu (S.H.), richard.zimmermann@uks.eu (R.Z.)
https://doi.org/10.1016/j.celrep.2018.03.122

SUMMARY

Protein transport into the mammalian endoplasmic reticulum (ER) is mediated by the heterotrimeric Sec61 channel. The signal recognition particle (SRP) and TRC systems and Sec62 have all been characterized as membrane-targeting components for small presecretory proteins, whereas Sec63 and the lumenal chaperone BiP act as auxiliary translocation components. Here, we report the transport requirements of two natural, small presecretory proteins and engineered variants using semipermeabilized human cells after the depletion of specific ER components. Our results suggest that hSnd2, Sec62, and SRP and TRC receptor each provide alternative targeting pathways for short secretory proteins and define rules of engagement for the actions of Sec63 and BiP during their membrane translocation. We find that the Sec62/Sec63 complex plus BiP can facilitate Sec61 channel opening, thereby allowing precursors that have weak signal peptides or other inhibitory features to translocate. A Sec61 inhibitor can mimic the effect of BiP depletion on Sec61 gating, suggesting that they both act at the same essential membrane translocation step.

INTRODUCTION

In eukaryotic cells, the endoplasmic reticulum (ER) membrane is a major site of protein biogenesis and the entry point into the compartments of the exocytic and endocytic pathways and the extracellular space (Dudek et al., 2015). Transport of the precursors of soluble polypeptides, such as presecretory proteins, into the mammalian ER typically involves amino terminal signal peptides in the precursors and transport components in the cytosol, ER membrane, and ER lumen. Transport involves at least three discreet stages, which can occur co- or post-translationally: (1) targeting of the precursor to the heterotrimeric Sec61 complex in the ER membrane; (2) insertion of the precursor into the Sec61 complex and simultaneous opening of the polypeptide conducting channel; and (3) completion of translocation. Early in translocation, the signal peptides are typically cleaved off by signal peptidase. In the case of glycoprotein precursors, N-glycosylation of asparagine residues within the mature regions is mediated by oligosaccharyl transferase. Therefore, monitoring these two modifications provides information on transport.

Signal peptides are typically about 25 amino acid residues long and have a three-domain structure with a positively charged amino terminus (N region), a central region containing hydrophobic residues (H region), and a slightly polar C terminus (C region; von Heijne, 1985; Hegde and Bernstein, 2006). Although signal sequences lack homologous sequence motifs, they have a dual function; they target presecretory proteins to the Sec61 complex and trigger the opening of a polypeptide-conducting channel within the Sec61 complex for passage of the polypeptide to the ER lumen (Görlich and Rapoport, 1993; Wirth et al., 2003; Dejgaard et al., 2010; Conti et al., 2015). In co-translational transport, signal peptides are recognized by a cytosolic signal recognition particle (SRP) when they emerge from ribosomes, and the ribosome/SRP/nascent chain complexes are targeted to Sec61 complexes via heterodimeric SRP receptor (SR) in the ER membrane. The hydrophobic core of signal sequences is primarily responsible for recognition and binding by SRP; positively charged side chains in the N region fine-tune SRP binding (Nilsson et al., 2015). In post-translational transport, ER membrane protein Sec62 has been suggested to act as a targeting receptor for small presecretory proteins with comparatively short and apolar signal peptides (Lakkaraju et al., 2012; Lang et al., 2012). The hydrophobicity of the H region was found to be crucial for Sec61 channel gating to the open state, and positively charged side chains in the N region and early part of the mature region have a major impact on the orientation of the signal sequence in the polypeptide-conducting channel (Nilsson et al., 2015). The hydrophobicity of the H region is supposed to be recognized by a so-called "hydrophobic patch" in transmembrane helices 2 and 7 of the α-subunit of the Sec61 complex, which form the so-called lateral gate of the polypeptide-conducting channel for the movement of signal peptides into the phospholipid bilayer (Voorhees and Hegde, 2016). Though some signal peptides may be "strong" enough to trigger Sec61 channel opening on their own (or during simultaneous priming by the ribosome in co-translational transport), such as

the preprolactin signal sequence, there are others, such as the signal sequences of the precursors of prion protein or ERj3, that require help from auxiliary transport components, such as BiP, Sec62, and Sec63 (Lang et al., 2012; Schäuble et al., 2012; Davis et al., 2015; Conti et al., 2015). The distinction between strong and "weak" signal peptides with respect to Sec61 channel gating and their putative link to the required auxiliary components remain elusive.

Post-translational transport of presecretory proteins into the mammalian ER was first reported for a couple of small exotic presecretory proteins, such as preprocecropin A (Schlenstedt et al., 1990; Schlenstedt and Zimmermann; 1987; Müller and Zimmermann, 1987, 1988). Recently, small human presecretory proteins were described that can be post-translationally transported into the mammalian ER (Shao and Hegde, 2011; Lakkaraju et al., 2012; Johnson et al., 2012), and post-translational transport of preprocecropin A into the ER was observed in intact human cells (Shao and Hegde, 2011). Subsequently, the combination of small interfering RNA (siRNA)-mediated gene silencing and protein transport into the ER of semi-intact human cells showed that post-translational transport of preprocecropin A into the human ER occurs independently of the SRP targeting system and involves the ER membrane proteins Sec62 and Sec63 (a Hsp40-type co-chaperone), as well as the ER lumenal Hsp70-type chaperone BiP (Lang et al., 2012; Schäuble et al., 2012; Johnson et al., 2013). Furthermore, post-translational ER targeting of several small human precursor polypeptides into the human ER has been reported to occur independent of SRP and to involve cytosolic transmembrane recognition complex (TRC)40 or Sec62 (Lakkaraju et al., 2012; Johnson et al., 2013). From these studies, the concept emerged that Sec62 and the TRC system comprising TRC40 in the cytosol and the Wrb/Caml heterodimer in the ER membrane may act as alternative signal peptide receptors in post-translational ER protein targeting. Meanwhile, yet another SRP-independent ER targeting pathway was discovered in yeast, the SRP–independent (SND) pathway, which was shown to involve an ER membrane protein with a human ortholog, hSnd2 (Aviram et al., 2016; Haßdenteufel et al., 2017).

Here, we addressed several of these issues utilizing two small human presecretory proteins and the established combination of siRNA-mediated gene silencing and protein transport into the ER of semi-intact human cells (Lang et al., 2012). Specifically, we addressed the following questions by studying a variety of predesigned precursor polypeptides, including signal sequence swap variants and dihydrofolate reductase (DHFR) hybrids, as well as mutated mature regions: which targeting and transport components are involved in ER import and which feature(s) of precursor polypeptides, signal peptides, and mature regions determine their engagement. Our results are consistent with and update the view that hSnd2, Sec62, SRα, and Wrb/Caml are involved in alternative targeting pathways for small presecretory proteins to the Sec61 complex. With respect to Sec61 channel gating, the data strongly suggest that BiP and Sec63, together with Sec62, facilitate Sec61 channel gating to the open state when small precursor polypeptides with weak signal peptides and detrimental features in the mature region are targeted. Interestingly, the precursor-specific transport defect after BiP depletion is mimicked by a heptadepsipeptide-type Sec61 inhibitor, which is also known to act in a precursor-selective manner (Mackinnon et al., 2014). Therefore, we suggest that BiP supports the same essential step in Sec61 gating that is inhibited by heptadepsipeptides.

RESULTS

Depletion of hSnd2 and TRC Receptor Inhibits Targeting of Prestatherin to the Sec61 Complex

To identify ER-membrane-resident targeting components of the small presecretory proteins, such as hSnd2 and Wrb/Caml, we studied their transport into the human ER by the established combination of siRNA-mediated gene silencing in HeLa cells and *in vitro* transport into the ER of semipermeabilized cells. Sec61 complex and SRα depletion served as positive controls for ER import and targeting, respectively (Lang et al., 2012; Johnson et al., 2013). Typically, the cells were converted to semipermeabilized cells by digitonin treatment and employed in transport reactions in rabbit reticulocyte lysate without or after inhibition of protein synthesis (i.e., under co- or post-translational conditions). The lysates were programmed with mRNAs encoding preproapelinOPG2 (ppa) or prestatherinOPG2 (ps) in the presence of [^{35}S]methionine and incubated with varying amounts of semipermeabilized cells that were in the linear range of the assay (Figures 1A–1C, S1A, and S1B; Tables S1 and S2). The presecretory protein, preprolactin (ppl) (SR dependent and Sec61 dependent) and the tail-anchored model protein Sec61ßOPG1 (Wrb/Caml dependent and Sec61 independent) were analyzed as controls (Figures 1A, 1B, and 1D; Lang et al., 2012; Johnson et al., 2012). Subsequently, all samples were subjected to SDS-PAGE and phosphorimaging. As an indication of transport efficiency, signal peptide cleavage (all three presecretory proteins) and/or N-glycosylation (all three proteins with OPG tag) were quantified and visualized in comparison to cells treated with the negative control siRNA (Figures S1C–S1F). Knockdown was evaluated by western blot with established antibodies (Figures S1G and S1H).

First, we depleted the Sec61 complex and observed the expected phenotypes. All three presecretory proteins (ppl, ppa, and ps) were substantially inhibited in their transport into the ER ($p < 0.01$ or < 0.5), but the membrane insertion of Sec61ßOPG1 was completely unperturbed (Figure 2A). Next, we selectively depleted SRα, hSND2, and Wrb by treating HeLa cells with established siRNAs and converted them to semipermeabilized cells. Subsequently, the various semi-intact cells were present during synthesis of the paradigm SRP-dependent precursor protein ppl or incubated with the model tail-anchored membrane protein Sec61ßOPG1. Though depletion of SRα led to inhibition of ppl transport into the ER as expected, hSnd2 depletion by an established siRNA stimulated ppl transport ($p < 0.05$; Figures 2B and 2C). This stimulation was consistent with elevated levels of SRα ($p < 0.05$; Figure 2E). Membrane integration of Sec61ßOPG1, which was measured as N-glycosylation, was unperturbed by both manipulations, demonstrating that SRα and hSnd2 knockdown did not grossly affect ER integrity and that comparable levels of ER membranes were present in the assays (Figures 2B and 2C). The opposite phenotype was observed after Wrb depletion (measured as Caml depletion),

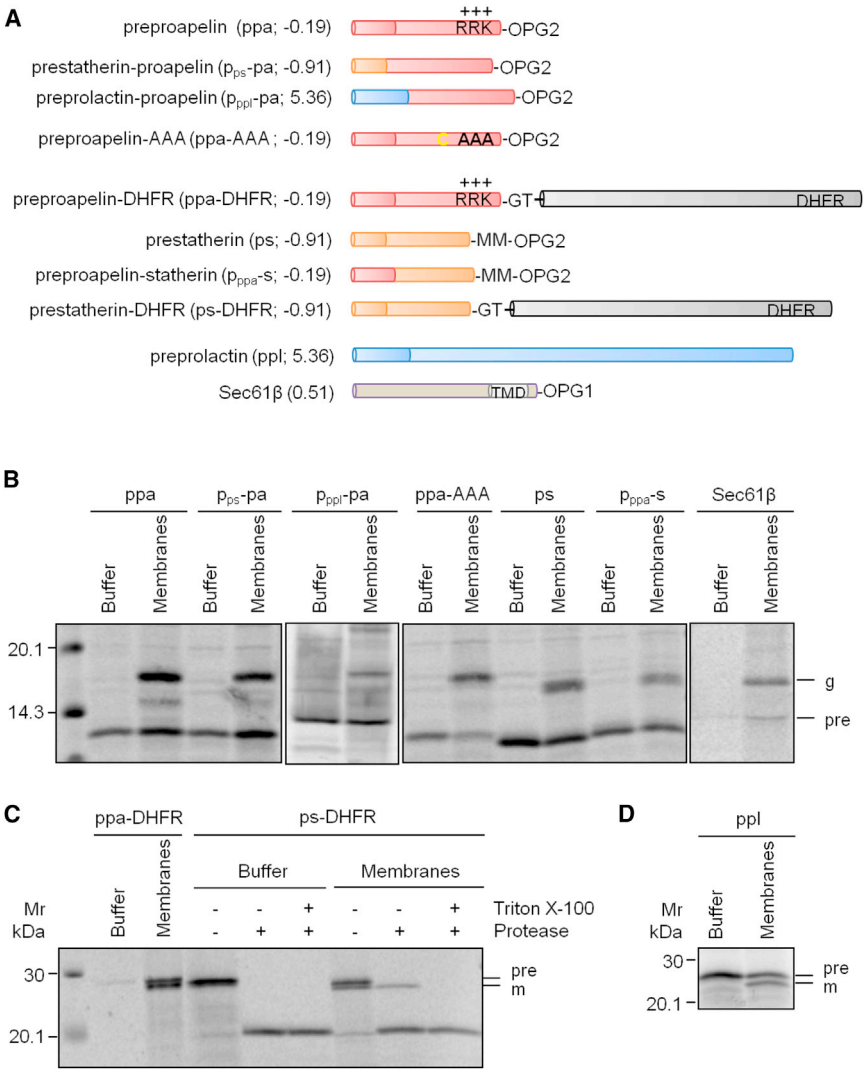

Figure 1. Model Precursor Proteins

(A) Precursor proteins were C-terminally extended or mutagenized in the signal peptide or mature region, as indicated. Numbers refer to predicted ΔG values for signal peptide or TMD (http://dgpred.cbr.su.se). TMD, transmembrane domain.

(B) Synthesis of the OPG2-tagged precursor polypeptides ppa plus its indicated variants, ps plus its indicated variant, and Sec61ßOPG1 in reticulocyte lysate in the absence (i.e. presence of buffer) or presence of ER membranes.

(C) Synthesis of the DHFR variants of precursor polypeptides ppa and ps in reticulocyte lysate in the absence (i.e. presence of buffer) or presence of ER membranes and subsequent treatment with proteinase K and Triton X-100.

(D) Synthesis of the precursor polypeptide ppl in reticulocyte lysate in the absence (i.e. presence of buffer) or presence of ER membranes.

All samples in (B)–(D) were subjected to SDS-PAGE (in parallel to radioactive mass standards) and phosphorimaging. Shown are relevant parts of phosphorimages. g, glycosylated protein; m, mature protein; pre, precursor polypeptide.

See also Figure S1 and Tables S1 and S2.

ppl processing was unperturbed, and N-glycosylation of Sec61ßOPG1 was partially inhibited ($p < 0.01$; Figure 2C).

With respect to N-glycosylation of the small presecretory proteins, hSnd2 depletion had a significant effect only on the post-translational transport of ps ($p < 0.05$), though the knockdown efficiencies were >90% (Figures 2C and 2E). Knockdown of Wrb to ~10% of the content in control cells led to a similar phenotype, i.e., had a considerable effect only on ps under post-translational conditions. Furthermore, the combination of *hSND2* with *WRB* siRNA was notably more harmful to ps transport than when used separately ($p < 0.05$). Thus, the additive effect on ps translocation upon simultaneous depletion of hSnd2 and Wrb must be due to a loss of both targeting pathways. In contrast, ppa did not appear to be able to efficiently use either of these two pathways. At depletion efficiencies of ~90%, both small presecretory proteins were transported into the ER less efficiently at low SRα levels under both experimental conditions (Figures 2B and 2E). The effects of SRα depletion were more pronounced under co-translation conditions than post-translational conditions ($p < 0.001$ for ps) and stronger for ps than ppa ($p < 0.01$).

These results are consistent with hSnd2 Wrb and SRα being involved in alternative targeting pathways and SRP and SR facilitating even post-translational protein transport into the human ER. Furthermore, these data suggest that ps, despite its smaller overall size, is better suited to engage the SRP/SR system for ER targeting than ppa, which correlates with higher hydrophobicity (i.e., lower ΔG^{pred}) of its signal peptide (Figure 1A). However, a significant proportion of SRP-independent transport of these small presecretory proteins is demonstrated to occur under co-translational assay conditions, reiterating the notion that small presecretory proteins represent one class of precursors targeted to the ER in an SRP/SR-independent manner and that the overall size of precursor proteins may be a crucial feature determining the targeting mechanism (Schlenstedt et al., 1990). To experimentally address this point, ppa and ps were extended at their C termini via fusion with DHFR (Figures 1A and 1C) and the transport requirements of these non-natural precursor polypeptides analyzed (Figure 2B). Transport of ppa-DHFR and ps-DHFR occurred only under co-translational conditions (Figure 1C versus S1I), consistent with precursor size being one determining factor for ribosome dependence of transport.

Depletion of Sec62 Inhibits Targeting of Preproapelin and Prestatherin to the Human ER

Post-translational ER targeting of several small human precursor polypeptides into the human ER has been reported to involve

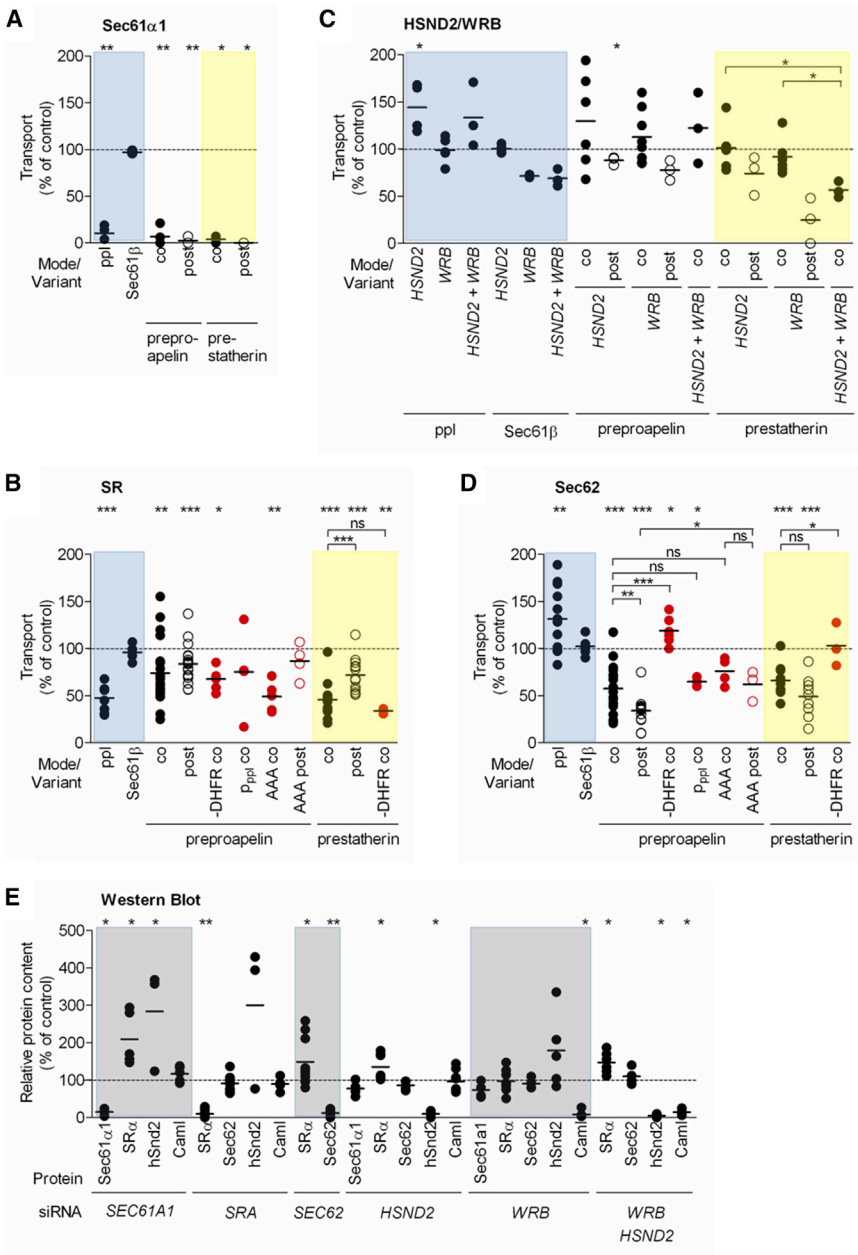

Figure 2. Targeting of Small Human Presecretory Proteins to the Sec61 Complex in the ER Membrane Involves Various Pathways

(A) Effects of Sec61α1 depletion on transport of ppl, Sec61ß, ppa, and ps under co- or post-translational conditions.

(B) Effects of SR depletion on transport of ppl, Sec61ß, ppa plus variants (in red), and ps plus variants under co- or post-translational conditions.

(C) Effects of HSND2 and/or Wrb depletion on transport of ppl, Sec61ß, ppa, and ps under co- or post-translational conditions.

(D) Effects of Sec62 depletion on transport of ppl, Sec61ß, ppa plus variants (in red), and ps plus variants under co- or post-translational conditions.

(E) Protein content of the indicated HeLa cells relative to β-actin was validated by western blot using the indicated antibodies and the control sample was set to 100%.

In (A)–(D), prior to preparation of semi-permeabilized cells, HeLa cells were treated with the indicated siRNA(s) (Table S3). Precursors were co- (co) or post-translationally (post) incubated with the indicated ER membranes. Radioactive samples were subjected to SDS-PAGE and phosphorimaging. Targeting efficiencies were calculated as the proportion of N-glycosylation and/or signal peptide cleavage of the total amount of synthesized precursors with the control sample set to 100%.

Shown are individual data points of at least three independent experiments and the mean. Statistical significance (***$p < 0.001$, **$p < 0.01$, *$p < 0.05$) was tested by Student's t test (upper panel) or using ANOVA plus post hoc Dunnett or Newman-Keuls multiple comparison test (horizontal brackets).

See also Figure S2.

Sec62 (Lakkaraju et al., 2012; Johnson et al., 2013), leading to the concept that Sec62 may act as alternative signal peptide receptor in post-translational ER protein targeting. Therefore, the effects of Sec62 depletion were analyzed following the established protocol. Co-translational transport of ppl and post-translational membrane insertion of Sec61ßOPG1 were completely unaffected by Sec62 knockdown (Figures 2D and 2E). At depletion efficiencies of ~90%, both small presecretory proteins were transported into the ER less efficiently at low Sec62 levels under both experimental conditions (Figures 2D and 2E). The effects of Sec62 knockdown were stronger for ppa ($p < 0.05$) and more pronounced under post-translational conditions ($p < 0.05$). Notably, knocking down Sec62 led to SRα overproduction ($p < 0.05$; Figure 2E), which may have compensated for Sec62 depletion under conditions of co-translational transport (Figure 2D). Therefore, this effect may have led to an underestimation of the effects of Sec62 knockdown on the small presecretory proteins, particularly under co-translational transport conditions. In contrast to their small counterparts, ppa-DHFR and ps-DHFR phenocopied ppl, i.e., did not show a requirement of co-translational transport for Sec62 (Figure 2D). This is consistent with Sec62 acting as a receptor of fully synthesized small precursor polypeptides (Lakkaraju et al., 2012) but does not rule out that Sec62 also facilitates Sec61 channel gating.

Depletion of Sec63 Inhibits Translocation of Preproapelin and Prestatherin into the Human ER

Having identified a role for Sec62 during the transport of our small-model presecretory proteins into the human ER, we addressed the contribution of Sec63, a known Sec62 interaction partner

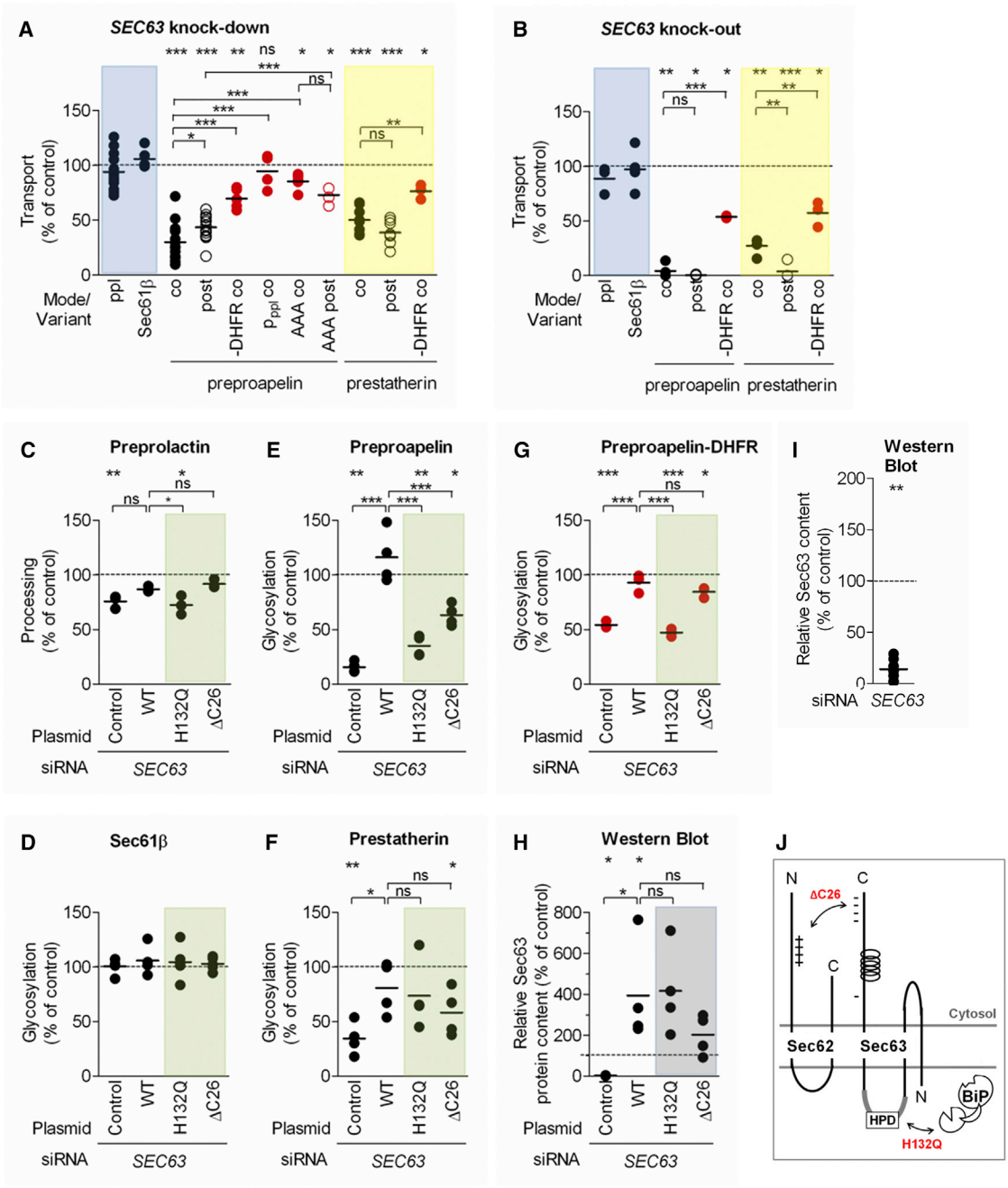

Figure 3. Translocation of Small Human Presecretory Proteins into the ER Lumen Involves Sec63

(A) *SEC63* siRNA effects on ppl, Sec61β, ppa, ps, and respective variants.

(B) Murine *SEC63* knockout effects on ppl, Sec61β, ppa, ps, and DHFR hybrids.

(C–H) Plasmid complementation of *SEC63* siRNA effects.

(C) ppl.

(D) Sec61β.

(E) ppa.

(F) ps.

(G) ppa-DHFR.

In (A)–(G), HeLa cells were transfected with SEC63-UTR siRNA and the indicated plasmids. Precursors were co- or post-incubated with the indicated ER membranes and analyzed by SDS-PAGE and phosphorimaging.

(legend continued on next page)

that is believed to regulate Sec61 activity (Dudek et al., 2015). Following our established protocol, the effects of Sec63 depletion were analyzed. A 90% depletion of Sec63 (Figure 3I) resulted in the substantially reduced transport of both small presecretory proteins into the ER, irrespective of whether the experiments were performed co- or post-translationally ($p < 0.001$ each; Figure 3A). In contrast, the transport of ppl and membrane insertion of Sec61ßOPG1 were unaffected by Sec63 knockdown (Figure 3A), and we conclude that the membrane translocation of the two small presecretory proteins shows a selective requirement for Sec63.

Because these were the first experiments addressing the Sec63 involvement in the translocation of small human presecretory proteins into the mammalian ER, two additional established experimental strategies were used: complementation of the siRNA knockdown by the respective cDNA and the use of murine *SEC63*-knockout cells (Lang et al., 2012; Fedeles et al., 2011). When transport of ppa and ps into the ER of *SEC63*$^{-/-}$ cells was analyzed in comparison to *SEC63*$^{+/+}$ cells, almost full inhibition of transport of both small presecretory proteins occurred under both experimental conditions (Figure 3B). Notably, a significant proportion of ribosome-independent transport may have occurred under co-translational conditions. In contrast, ppl and Sec61ßOPG1 were unaffected. For complementation of *SEC63* siRNA effects, HeLa cells were simultaneously treated with *SEC63*-UTR siRNA and *SEC63* expression plasmid or the corresponding vector. Next, the cells were converted to semipermeabilized cells and the transport of various precursors analyzed. Again, ppl and Sec61ßOPG1 served as controls (Figures 3C and 3D). In contrast to the vector control, efficient expression of *SEC63* in the presence of *SEC63* siRNA fully restored co-translational transport of the two small presecretory proteins, which demonstrates that the Sec63 knockdown effects were specific (Figures 3E, 3F, and 3H). Thus, transport of the two small presecretory proteins into the ER does indeed involve Sec63. Upon closer inspection of the Sec63 knockout data (Figure 3B), it was apparent that ps translocation is more dependent upon Sec63 when its transport is post-translational than when it is co-translational ($p < 0.01$). Because ps is shorter than ppa, these data appear to support the notion that the overall size of a precursor protein is a crucial feature in determining its dependency on Sec63. In order to experimentally address this point, the transport requirements of ppa-DHFR and ps-DHFR were also analyzed. Although these hybrid precursors still required Sec63 for efficient co-translational transport into the murine ER ($p < 0.05$ each; Figures 3A and 3B), the loss of Sec63 had much less of an effect than that observed with their smaller counterparts ($p < 0.001$ and $p < 0.01$). Thus, the small size of the precursors is one, but not the sole, determinant for its Sec63 requirement and ribosome-dependent transport is supported by Sec63 too. In order to consider the contribution of other properties, such as the signal sequence, the transport of a chimera composed of the ppl signal peptide preceding the mature region of proapelin (p_{ppl}-pa) was analyzed for its Sec63 requirement (Figure 3A). The p_{ppl}-pa phenocopied ppl, i.e., did not require Sec63 for its co-translational transport into the ER.

The successful complementation of *SEC63* siRNA phenotypes by *SEC63* cDNA allowed us to analyze Sec63 mutant variants with a deletion of 26 negatively charged amino acids in the cytosolic C terminus, which prevents Sec62 interaction, or a point mutation in the characteristic histidine-proline-aspartate (HPD) motif in the ER lumenal J-domain, which mediates BiP interaction (Figures 3H and 3J; Müller et al., 2010; Schäuble et al., 2012). When the effects of Sec63H132Q or Sec63ΔC26 overproduction were analyzed in the presence of *SEC63*-UTR siRNA, different phenotypes were observed for the two presecretory proteins. In the case of ps, the Sec63 mutants were as fully active in restoring transport, whereas in the case of ppa, the Sec63H132Q mutant was almost completely inactive and Sec63ΔC26 only partially restored co-translational transport (Figures 3E and 3F). First, this suggests a possible differential effect of BiP in the transport of the two small presecretory proteins, which will be discussed below. Second, Sec62 and Sec63 may cooperate in facilitating the translocation of ppa into the mammalian ER, i.e., Sec61 channel opening. In the case of ps, even though the two proteins function as a heterodimeric complex, Sec63 appears to additionally have an intrinsic function in Sec61 channel gating. Thus, the differential requirement for Sec63/Sec62 and Sec63/BiP interaction suggests three independent and substrate-specific functions of Sec63, one in cooperation with Sec62 or BiP (only for ppa), and one intrinsic function (at least for ps). These conclusions were further substantiated by the behavior of ppa-DHFR, which depends on SRα, but not Sec62, for targeting. After Sec63 knockdown, transport of the hybrid precursor was efficiently restored by wild-type Sec63 and Sec63ΔC26, but not Sec63H132Q (Figure 3G).

Depletion of BiP Inhibits Translocation of Preproapelin, but Not Prestatherin

Short subtilase cytotoxin SubAB treatment is the method of choice for BiP depletion in HeLa cells, providing an acute and highly efficient depletion while maintaining robust cell viability (Paton et al., 2006; Schäuble et al., 2012). HeLa cells were treated for 2 hr with SubAB or the inactive variant $SubA_{A272}B$, semipermeabilized, and the transport of the small presecretory proteins analyzed. At 95% depletion efficiency, ppa transport was much more efficiently inhibited by the active toxin than ps transport ($p < 0.001$ and < 0.01 for ppa), whereas ppl and Sec61ßOPG1 were unaffected (Figures 4A and 4I). Similar observations were made after BiP depletion using siRNA ($p < 0.05$; post-translational), an alternative though less efficient depletion strategy (Figures 4B and 4I). Thus, BiP plays a substrate-specific role in the translocation of small presecretory

(H) Sec63 protein content of the HeLa cells, complemented as indicated, relative to β-actin was validated by western blot and the control sample was set to 100%.
(I) Sec63 protein content of HeLa cells, depleted as indicated, relative to β-actin was validated by western blot and the control sample was set to 100%.
(J) Sec63 interactions and *SEC63* mutants (red) used in the complementation assay.
Shown are individual data points of at least three independent experiments and the mean. Statistical significance (***$p < 0.001$, **$p < 0.01$, *$p < 0.05$) was tested by Student's t test (upper panel) or using ANOVA plus post hoc Dunnett or Newman-Keuls multiple comparison test (horizontal brackets).
See also Figures S2 and S3.

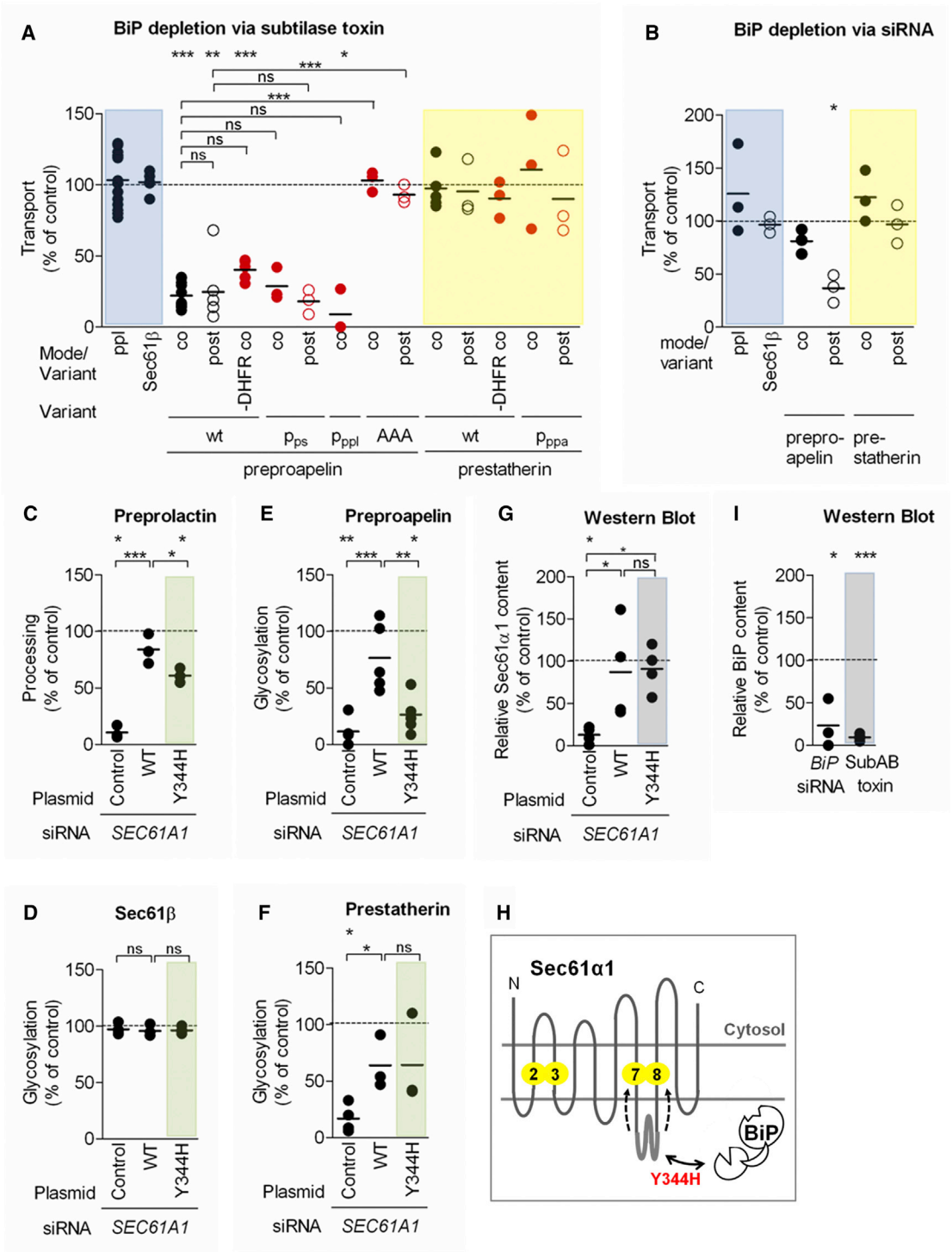

Figure 4. Selective Effects of BiP Depletion and Sec61 Mutation on the Translocation of Two Small Human Presecretory Proteins into the ER Lumen

(A) Subtilase toxin effects on ppl, Sec61β, ppa, ps, and respective variants.

(B) *BiP* siRNA effects on ppl, Sec61β, ppa, and ps.

(C–G) Complementation of *SEC61A1* siRNA effects.

(C) ppl.

(D) Sec61β.

(legend continued on next page)

proteins. This finding is perfectly in line with the differential effect of Sec63H132Q, which does not allow productive interaction with BiP. After knockdown of Sec63, this mutant restored the transport of ps, but not ppa (Figures 3E and 3F). In order to independently address this point, the transport of ppa-DHFR and ps-DHFR was analyzed. The hybrid precursor ppa-DHFR phenocopied ppa by showing a requirement for BiP in co-translational transport into the human ER ($p < 0.001$), whereas ps-DHFR behaved like ps and showed no requirement for BiP (Figure 4A). Thus, BiP plays a substrate-specific role in the translocation of small presecretory proteins that is unrelated to the overall size of the precursor protein.

Taken together, our data suggest that BiP and its co-chaperone Sec63 are simultaneously involved in the transport of ppa, but not ps (Figures 3A, 3B, 4A, and 4B). Because the role of Sec63 in short presecretory protein transport is strongly dependent upon the signal sequence (Figure 3A), we investigated whether this is also the case for BiP. Thus, p_{ppl}-pa and derivatives of ppa and ps with mutually exchanged signal peptides (p_{ps}-pa and p_{ppa}-s; Figure 1) were subjected to the transport assay after BiP depletion. Surprisingly, neither the ppl nor ps signal sequences enabled the BiP-independent translocation to proapelin, and likewise, the substitution of the ppa signal sequence did not result in BiP-dependent translocation for statherin (Figure 4A). Thus, the key feature of the requirement for BiP during membrane translocation is not the signal sequence.

Consequently, we shifted our scrutiny to the mature region of ppa and noted an interesting accumulation of basic amino acid residues located in its C-terminal region. The contribution of this region to the membrane transport requirements of ppa was addressed by mutating a continuous stretch of three basic residues to a triple alanine (Figure 1; Table S1). Strikingly, the resulting ppa-AAA behaved like ps, and it showed no requirement for BiP under either co- or post-translational conditions (Figure 4A). Thus, this cluster of three basic amino acid residues determines the BiP dependency of ppa translocation. The phenotype of ppa-AAA led us to re-examine whether the positive charges also contribute to the other requirements of ppa that we had identified, and we found that ppa-AAA was indeed less dependent on Sec62 and Sec63, but not SR, than the original ppa (Figures 2B, 2D, and 3A). In short, our data are consistent with the idea that Sec62, Sec63, and BiP all contribute to Sec61 channel opening but show that Sec62 and Sec63 respond to both the signal sequence and the mature region of small presecretory proteins; the actions of BiP that we observed are primarily driven by the mature region.

In order to better understand how BiP acts to promote ppa transport, we used a Sec61 mutant defective in BiP binding (Sec61α1Y344H) to rescue HeLa cells that had been depleted of endogenous Sec61α (Figures 4G and 4H; Lloyd et al., 2010; Schäuble et al., 2012). When the resulting cells were semipermeabilized and the transport of the small presecretory proteins analyzed, we found that ppa transport was sensitive to Sec61α1Y344H ($p < 0.05$), but ps transport was not (Figures 4E and 4F). This finding strongly supports our hypothesis that ppa insertion into the Sec61 channel requires the Sec63-mediated binding of BiP to ER lumenal loop 7 of the Sec61 α-subunit and that this interaction allows the productive insertion of ppa into the Sec61 channel.

Selective BiP Requirement Correlates with Heptadepsipeptide Sensitivity

Previous studies of heterologous model substrates suggest that the ability of the cyclic heptadepsipeptides CAM741 to inhibit the Sec61-mediated translocation of small presecretory proteins is strongly dependent upon the signal sequence (Johnson et al., 2013; Mackinnon et al., 2014). For other precursor proteins, however, adjacent residues in the mature region were also shown to be relevant. We therefore, explored the effect of CAM741 (25 μM) on the ER translocation of our two model small presecretory proteins and found ppa transport to be much more sensitive to this inhibitor than ps under both co- and post-translational conditions ($p < 0.001$ and < 0.01; Figure 5). The ppa-DHFR ($p < 0.05$) and ps-DHFR hybrids phenocopied their small counterparts, whereas ppl and Sec61ßOPG1 were unaffected by inhibitor treatment (Figure 5). Only the BiP-independent variant of ppa, ppa-AAA, with charge depletion at its C terminus, resulted in a CAM741 insensitive precursor (Figure 5), providing convincing evidence that properties far within the mature region of a precursor protein can influence CAM741 sensitivity. Moreover, the CAM741 sensitivity and BiP dependence of ppa and ppa-AAA clearly correlated. Thus, the role of BiP in modulating Sec61 channel gating coincides with the substrate-specific inhibition of protein translocation by CAM741.

Absence of Sec62, Sec63, or BiP and Presence of Heptadepsipeptide Inhibitor Trap Preproapelin at the Cytosolic Face of the Sec61 Channel

Regarding a putative Sec61 gating function of auxiliary components (Sec62, Sec63, and BiP), we assumed that, if they indeed facilitate opening of the Sec61 channel, then their depletion would trap precursor polypeptides at the translocon, similarly to heptadepsipeptide inhibitors (Mackinnon et al., 2014). To test this hypothesis, we used the cysteine-reactive homobifunctional reagent bismaleimidohexane (BMH) for chemical cross-linking of fully synthesized ppa. Importantly, ppa contains its only two cysteine residues, both located within the signal

(E) ppa.
(F) ps.
In (A)–(F), HeLacells were treated with the indicated siRNA, plasmid, or subtilase toxin.Precursors were co or post incubated with the indicated ER membranes andanalyzed by SDS-PAGE and phosphorimaging.
(G) Sec61α protein content of the HeLa cells, complemented as indicated, relative to β-actin was validated by western blot and the control sample was set to 100%.
(H) BiP interaction with Sec61α1-loop 7 and the mutant (red) used in the complementation assay. HeLa cells were treated with the indicated siRNA, plasmid, or subtilase toxin. Precursors were co or post incubated with the indicated ER membranes and analyzed by SDS-PAGE and phosphorimaging.
(I) BiP protein content of the HeLa cells, depleted as indicated, relative to β-actin was validated by western blot and the control sample was set to 100%.
Shown are individual data points of at least three independent experiments and the mean. Statistical significance (***$p < 0.001$, **$p < 0.01$, *$p < 0.05$) was tested by Student's t test (upper panel) or using ANOVA plus post hoc Dunnett or Newman-Keuls multiple comparison test (horizontal brackets).
See Figure S4.

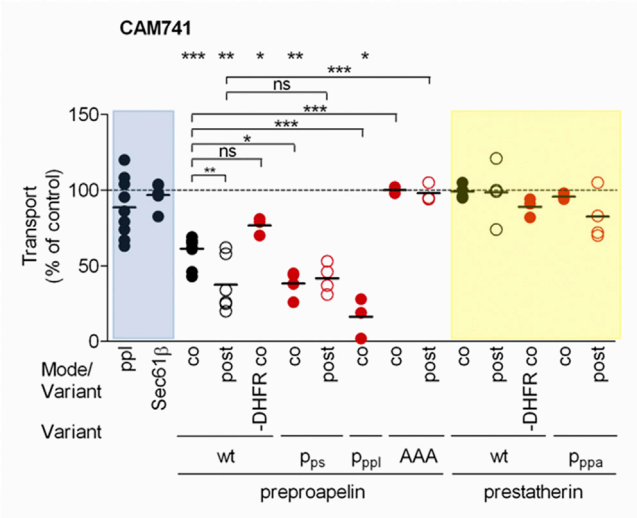

Figure 5. Selective Effects of a Cyclic Heptadepsipeptide Inhibitor on the Translocation of Preproapelin and Preprostatherin into the ER Lumen

CAM741 effects on ppl, Sec61β, ppa, ps, and respective variants. Precursors were co- or post- incubated with canine pancreatic rough microsomes after pretreatment in the presence of solvent or CAM741 (25 μM) for 30 min at 0°C. Samples were subjected to SDS-PAGE and phosphorimaging.

Shown are individual data points of at least three independent experiments and the mean. Statistical significance (***$p < 0.001$, **$p < 0.01$, *$p < 0.05$) was tested by Student's t test (upper panel) or using ANOVA plus post hoc Dunnett or Newman-Keuls multiple comparison test (horizontal brackets).

See also Figure S5.

peptide (Table S1). Before crosslinking, ppa was co-translationally incubated with semipermeabilized HeLa cells depleted of Sec62, Sec63, or BiP or rough microsomes in the presence or absence of the CAM741. Under control conditions, crosslinking of ppa to Sec61α and Sec61β was hardly seen (Figure 6A, lanes 9, 14, and 19). Crosslinking to Sec61α and Sec61β was increased in the absence of Sec62 (lane 5), Sec63 (lane 7), and BiP (lane 12) and to Sec61α in the presence of CAM741 (lane 17). This was not the case for SRα, which facilitates targeting only (Figure 6A, lane 3). Strikingly, ppl and ppa-AAA did not show crosslinking under any of the analyzed conditions (Figures S6E–S6G). The identities of the Sec61α- and Sec61β-crosslinking products of ppa were verified by (1) immunoprecipitation under non-native (Figure 6B) as well as native, i.e., Sec61 complex-preserving, conditions (Figure 6C) and simultaneous absence when crosslinking was carried out after ppa import into Sec61α-depleted ER (Figures S6A and S6B) and (2), in case of the Sec61α-crosslinking product, by shift toward a higher molecular weight, in accordance with the expression of tagged variant and simultaneous depletion of the endogenous counterpart (Figures S6C and S6D). Thus, the absence of Sec61 modulators appeared to provoke accumulation of ppa at the translocon as a result of defective Sec61 channel opening (Figure 6D).

In order to further characterize the site of ppa accumulation at the Sec61 channel in the absence of the auxiliary components, we probed accessibility of accumulated ppa as well as its crosslinking products by externally added protease. Following either translocation or translocation plus crosslinking, membranes were re-isolated by centrifugation and treated with proteinase K (20 μg/mL) for 60 min at 0°C in the absence or presence of Triton X-100 (2%). After inhibition of proteolysis, all samples were analyzed by SDS-PAGE and phosphorimaging. Accumulated ppa as well as its Sec61α- and Sec61β-crosslinking products were protease sensitive, even in the absence of detergent (Figure S7). In contrast, pa was protease resistant in the absence of detergent but sensitive in the presence of detergent (Figures S7D and S7E), demonstrating the integrity of the ER under conditions of proteolysis in the absence of detergent. Thus, ppa accumulated outside of the ER, in general, and at the cytosolic face of the Sec61 channel, in particular, in the absence of auxiliary components. Because the unassigned crosslinking products were also protease sensitive in the absence of detergent (Figures S7A and S7C), they must represent adducts of ppa with cytosolic or ER membrane proteins.

DISCUSSION

Human cells secrete a large number of small proteins, which typically function as hormones or in pathogen defense. It is generally accepted that small human presecretory proteins can be post-translationally imported into the ER via the polypeptide-conducting Sec61 channel. We investigated the requirements of two small-model presecretory proteins (ppa and ps) for targeting to and translocation into the human ER and the features of the precursors that determine these requirements.

SR, TRC Receptor, hSnd2, and Sec62 Protein Are Involved in Alternative Pathways for Targeting Small Precursor Polypeptides to the ER

We observed that the human-model presecretory proteins ppa and ps can use Sec62, as well as SRα, for ER targeting, irrespective of the experimental conditions. Although smaller in overall size, ps (Table S2) apparently preferred SRα over Sec62-mediated targeting, whereas ppa did the opposite, which may be related to the higher hydrophobicity of the ps signal peptide (ΔG^{pred} −0.91 for ps versus −0.19 for ppa). We note that the mature region of ps comprises a C-terminally located peptide motif, which is reminiscent of the arrest peptide of XBP1 and may also have contributed to efficient SRP/SR involvement of this particular small presecretory protein (Table S1; Yanagitani et al., 2011). Taken together with our observation that C-terminal extension of ppa or ps by the cytosolic protein DHFR (187 amino acid residues) leads to Sec62 independence, the data presented support the hypothesis that small precursors use the SRP/SR system for ER targeting in mammalian cells less effectively, simply because the corresponding precursor polypeptide chains are more likely to be released from ribosomes before SRP can efficiently interact (Schlenstedt et al., 1990; Lakkaraju et al., 2012). Therefore, these precursors have to rely on alternative targeting systems, which can apparently involve Sec62. Notably, in yeast, low hydrophobicity of signal peptides and C-terminal signals for the attachment of glycosylphosphatidylinositol (GPI) anchors preclude effective use of SRP/SR and, therefore, cause

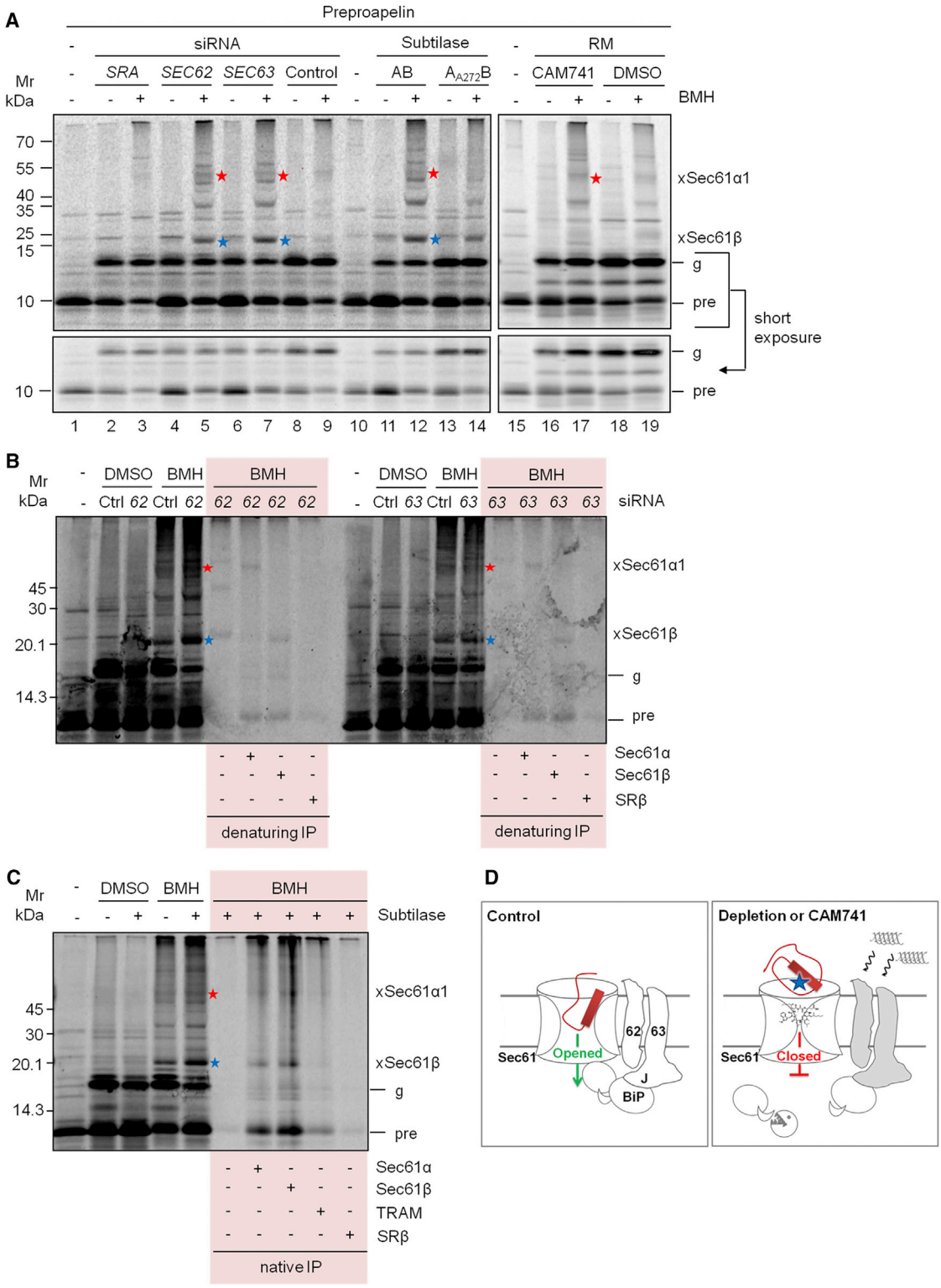

Figure 6. Sec62, Sec63, BiP, and CAM741 Act at an Early Stage of Protein Translocation

(A) Chemical crosslinking of ppa, followed by SDS-PAGE and phosphorimaging.

(B) Chemical crosslinking of ppa, followed by immunoprecipitaion with the indicated antibodies under denaturing conditions (where indicated) plus SDS-PAGE and phosphorimaging.

(legend continued on next page)

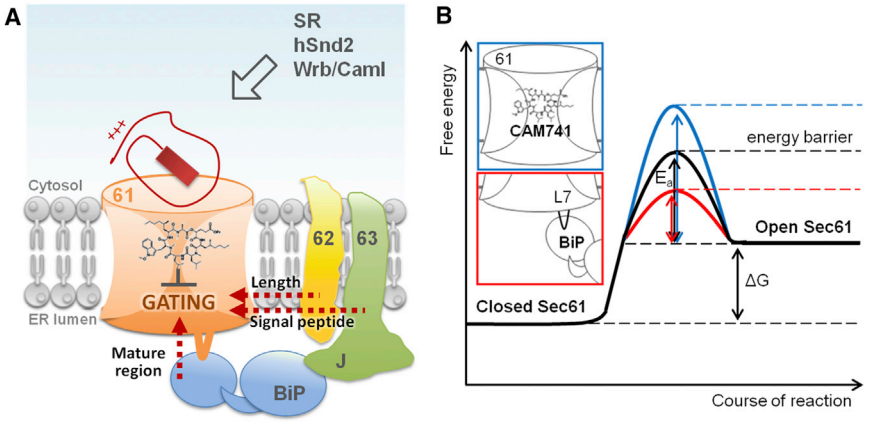

Figure 7. Model for Transport of Precursor Proteins into the Human ER

(A) Upon engagement of the precursor polypeptides with the translocon, the Sec61 channel is gated to the open state. Alternatively, unproductive interactions are sensed, each causing recruitment of different auxiliary components, such as BiP, Sec62, and Sec63, facilitating channel opening. Thereby, sampling of the channel interior is influenced by deleterious charges (ppa, red), hydrophobicity of the signal peptide, and mature region length. BiP overcomes CAM741-reinforced energy barrier for channel opening.

(B) Energy diagram for Sec61 channel gating.

Sec62p and GET dependence, respectively (Aviram and Schuldiner, 2014). In addition to SR and Sec62, co- and post-translational targeting of our two model presecretory proteins can also involve both the TRC system and the recently identified SND pathway, albeit to different degrees for the two different precursors (Figure 7A).

Sec63 Mediates the Translocation of Small Precursor Polypeptides into the ER in a Signal-Peptide-Specific Manner either by Itself or in Collaboration with Sec62 and/or BiP

Our observation that precursor polypeptides accumulate within the Sec61 channel upon Sec62, but not SRα, depletion suggested an additional Sec61 gating function for Sec62 in the absence of the ribosome. Indeed, in cases like ps, gating may be the only function of Sec62. However, Sec62 may also play a role in proper positioning of transmembrane helices in the Sec61 channel (Reithinger et al., 2013).

Here, the small presecretory protein ps presented us with a remarkable phenotype, as it apparently involves Sec63 and Sec62 independent of their contact, and it does so independently of BiP. Thus, Sec63 itself contributes to Sec61 channel gating, i.e., without involving BiP, most likely via its interaction with Sec61 complex. In the case of ps, this did not occur in collaboration with Sec62 as it does in the case of ppa, and this is supported by Sec62 independently translocating DHFR hybrids. This intrinsic activity of Sec63 was previously observed for Sec62-independent membrane integration of aquaporin 2 and invariant chain (Lang et al., 2012). Considering multiple Sec63 functions, the question arises of which features of ppa or ps actually determine its dependence on the function of Sec63 in Sec61 channel gating. The relevant feature determining the Sec63/BiP requirement is related to BiP dependence. Signal sequence swap variant p_{ppl}-pa suggests that the signal sequence contributes fully to requiring Sec63, at least for Sec63/Sec62, and most likely intrinsic Sec63 function. Though there are signal peptides strong enough to trigger Sec61 channel opening on their own, such as the ppl signal sequence, others, like the signal sequence of ppa, require help from the auxiliary transport component Sec63 (Figure 7). This is consistent with the notion of common characteristics of respective signal peptides (Lang et al., 2012) defining those short in size and with apolar residues as weak in terms of requiring Sec63 (Table S2). This is in accordance with the precursors (e.g., prion protein and ERj3) stabilizing the association of mammalian Sec61, Sec62, and Sec63 and having the same requirements as seen here (Conti et al., 2015) as well as the hydrophobicity of the H region being crucial for Sec61 channel gating to the open state (Nilsson et al., 2015).

BiP and Its Co-chaperone Sec63 Mediate Sec61 Channel Gating in the Case of Small Presecretory Proteins with Inhibitory Mature Regions

In addition to its intrinsic activity in protein translocation, Sec63 acts as Hsp40-type co-chaperone for ER lumenal Hsp70-type chaperone BiP. The collaboration of Sec63 and BiP involves the characteristic HPD motif in the ER lumenal J-domain of Sec63 and the interacting surface of the ATPase domain of BiP. Previously, the combination of siRNA-mediated gene silencing and protein transport into the ER of semi-intact human cells showed that post-translational transport of preprocecropin

(C) Chemical crosslinking of ppa, followed by immunoprecipitaion with the indicated antibodies under native conditions (where indicated) plus SDS-PAGE and phosphorimaging.

In (A)–(C), prior to preparation of semipermeabilized cells, HeLa cells were treated with the indicated siRNA (Table S3) or subtilase cytotoxin. Rough microsomes were treated with solvent or CAM741. ppa was co-translationally incubated with the indicated ER membranes, which were sedimented and resuspended in XL buffer before crosslinking with BMH. Samples were subjected to SDS-PAGE and phosphorimaging. Relevant crosslinking products of ppa to Sec61α1 or Sec61β are indicated by red and blue asterisks. g, glycosylated pa; pre, ppa.

(B and C) Where indicated, immunoprecipitation with validated antibodies was carried out after crosslinking and membrane solubilization under denaturing (1% SDS) (B) or non-denaturing conditions (0.65% CHAPS and 0.4 M KCl; Tyedmers et al., 2000) (C).

(D) Schematic representation of ppa translocation under control conditions and upon depletion of Sec62, Sec63, or BiP by siRNA (waved arrows) or toxin (pacman) treatment or in the presence of CAM741.

See Figures S6 and S7.

A into the human ER involves Sec62 and Sec63 as well as BiP (Lang et al., 2012; Schäuble et al., 2012). Using the same approach, Sec63 and BiP dependence was observed for two co-translationally transported substrates, the precursors of the prion protein and ER lumenal co-chaperone ERj3. Therefore, our model for BiP and Sec63 action at the early stage of co-translational and post-translational protein translocation is that some precursors may not be sufficiently strong to shift the dynamic equilibrium of the Sec61 channel to the open state, possibly even during simultaneous priming by the ribosome in co-translational transport, and that this has to be supported by Sec63-mediated binding of BiP to the ER lumenal loop 7 of the Sec61α subunit (Lang et al., 2012; Schäuble et al., 2012; Dudek et al., 2015). This model was further substantiated by the requirements of ppa, which depended on Sec63 and BiP for efficient insertion into the Sec61 complex and/or Sec61 channel gating to the open state. Therefore, ppa was sensitive to the Sec63H132Q and Sec61α1Y344H mutations. In contrast, ps was not BiP dependent and not sensitive to the two mutations. Consequently, Sec63 and BiP depletion resulted in an accumulation of ppa within the translocon.

Though the signal peptide of ppa was identified as a feature determining Sec63 dependence, it appeared not to be associated with requiring BiP. Instead, the mature region contributed to the "weakness" of ppa in Sec61 channel gating. The mature region of ppa contains a cluster of three positively charged amino acid side chains near the C terminus that weakens its gating property and causes the requirement for support by BiP. BiP dependence and inhibitor sensitivity of ppa were both attributed to a cluster of positively charged amino acid residues within the mature region of ppa, which was underlined by observations that replacement of this cluster by alanines relieves both BiP dependence and inhibitor sensitivity. Therefore, we suggest that the weakness of the ppa signal peptide is exacerbated by the cluster of positively charged amino acid residues within the mature region and, therefore, requires additional support from BiP (Figure 7A). We suggest that such a positive cluster may favor "head-first" rather than "hairpin" insertion of the signal peptide into the Sec61 channel. Alternatively, it may pose a particularly high energetic barrier for loop insertion of the signal peptide into the Sec61 channel or Sec61 channel opening and that this barrier can be amplified by heptadepsipeptide inhibitors (Figure 7B).

The clusters of positive amino acid residues within the mature region of ppa contain the dibasic cleavage site for furin and play a role in interaction of the mature hormone with its receptor (Shin et al., 2013). Therefore, the BiP dependence of ppa compensates the deleterious effect of a cluster of charged residues within proapelin, which is required for maturation and subsequent biological activity.

A Working Hypothesis for the Import of Small Presecretory Proteins into the Human ER

Due to their size, some small human presecretory proteins cannot be efficiently targeted to the ER by the SRP/SR system. Instead, they are specifically delivered to the Sec61 complex in the ER membrane by the TRC or SND pathway or directly by the Sec62 protein. Subsequently, their signal peptides start sampling the cytosolic funnel of the Sec61 channel pore (Zhang and Miller, 2012). According to these simulations, dwell time in the Sec61 channel pore is influenced by deleterious charges, hydrophobicity, mature protein domain length, and translation speed (dependent on pause sites plus rare codons or hairpins in the mRNA and arrest peptides plus polyproline motifs in the polypeptide), the latter two of which can be expected to be affected by C-terminal extension by DHFR. As noted above, the mature sequence of ps indeed comprises a C-terminally located peptide motif, which may contribute to SRP/SR involvement of this particular small presecretory protein. Upon the interaction of a signal peptide and downstream sequences with the Sec61 complex, the channel may be gated to the open state (1), sense unproductive interactions, such as a weak signal peptide or interfering features within the mature region (e.g., cluster of positively charged residues), recruit BiP for channel gating (2), or sense terminally unproductive interactions and recruit proteases, such as the proteasome (3). One could best envision this as a triage occurring for nascent or fully synthesized precursor polypeptides at the Sec61 channel. In addition, the BiP-mediated Sec61 channel gating to the open state is probably best considered in analogy to an enzyme-catalyzed reaction. Accordingly, BiP reduces the energetic barrier for channel opening, which can apparently be reinforced by heptadepsipeptides (Figure 7B).

EXPERIMENTAL PROCEDURES

Materials

Enhanced chemiluminescence (ECL), ECL Plex goat anti-rabbit immunoglobulin G (IgG)-Cy5, and ECL Plex goat anti-mouse IgG-Cy3 conjugate were purchased from GE Healthcare. Goat anti-rabbit IgG-peroxidase conjugate and antibodies against β-actin were purchased from Sigma. Page Ruler Prestained Protein Ladder and [^{14}C] methylated Rainbow marker CFA755 were purchased from Thermo Scientific and Amersham Biosciences, respectively.

Rabbit antibodies were raised against the C-terminal (14-mer) or amino terminal IQ peptides (14-mer) of human Sec61α; the amino terminal peptides of human Sec61β (9-mer); the C-terminal peptides of human SRα (10-mer), SRβ (12-mer), Sec62 (11-mer), Sec63 (13-mer), or TRAM (12-mer); the amino terminal peptides of human BiP (12-mer); the C-terminal peptide of human hSnd2 (14-mer), and a mix of two peptides of human Caml (Haßdenteufel et al., 2017).

The plasmids coding for human ppaOPG2, psOPG2, and Sec61ßOPG1 coded for the respective presecretory or tail-anchored proteins plus one (OPG1) or two (OPG2) N-glycosylation sites at the C terminus (Johnson et al., 2012). Where indicated, the OPG2 regions were replaced by dihydrofolate reductase (DHFR) cDNA (Schlenstedt et al., 1990) and the coding region for linker dipeptide (Gly-Thr). Similarly, the signal peptide regions of ppaOPG2 and psOPG2 were mutually exchanged or, in the case of ppaOPG2, replaced by the region coding for ppl signal peptide. Site-directed mutagenesis was used for alanine substitution of a basic tripeptide (RRK) at positions 59–61 of ppaOPG2. Bovine ppl was used as a control (Schlenstedt et al., 1990).

Cell Culture

HeLa cells (German collection of Microorganisms and Cell Cultures [DSMZ] no. ACC 57) were cultivated at 37°C in DMEM (Gibco) containing 10% fetal bovine serum (FBS) (Biochrom) and 1% penicillin/streptomycin (GE Healthcare) in a humidified environment with a 5% CO_2 atmosphere. Sec63 control cells (derived from the *SEC63*floxed mouse) and *SEC63*-null cells were cultured in DMEM/Ham's F-12 medium containing 1% FBS, 1% Insulin-Transferrin-Selenium-X, 10 U/L mouse interferon-γ, 1 μg/L 3,3′,5-triiodo-L-thyronine, and 1% penicillin/streptomycin under humidified conditions at 33°C in a 5% CO_2 atmosphere (Fedeles et al., 2011; Lang et al., 2012). Cell growth was monitored using the Countess Automated Cell Counter (Invitrogen) according to the manufacturer's instructions.

Depletion of Cells by siRNA or Toxin Treatment

For gene silencing, 5.2×10^5 HeLa cells were seeded in a 6-cm culture plate in normal culture. For gene silencing, the cells were transfected with targeting siRNA (Table S3) or control siRNA (AllStars Negative Control siRNA; QIAGEN) to a final concentration of 15–30 nM using HiPerFect Reagent (QIAGEN) as described previously (Lang et al., 2012; Johnson et al., 2012). After 24 hr, the medium was changed and the cells transfected a second time. Silencing efficiencies were evaluated by western blot analysis using the corresponding antibodies and a mouse anti-β-actin antibody. The primary antibodies were visualized using goat anti-rabbit IgG-peroxidase conjugate and ECL, ECL Plex goat anti-rabbit IgG-Cy5, or ECL Plex goat anti-mouse IgG-Cy3 conjugate and the Fusion SL (peqlab) luminescence imaging system or the Typhoon-Trio imaging system in combination with Image Quant TL 7.0 software (GE Healthcare). BiP-depleted cells were obtained by treating HeLa cells with the subtilase cytotoxin SubAB, which specifically inactivates BiP, at a final concentration of 1 μg/mL for 2 hr (Paton et al., 2006; Schäuble et al., 2012). Control cells were treated with $SubA_{A272}B$, an inactive mutant form of SubAB.

Complementation Analysis

To rescue the phenotype after *SEC61A1* or *SEC63* silencing and characterize the Sec61α1-Y344H, Sec63H132Q, or Sec63ΔC26 mutants, the corresponding cDNA was inserted into the multi-cloning sites of a pCDNA3-IRES-GFP vector as described previously (Lang et al., 2012; Schäuble et al., 2012). To identify interaction partners in crosslinking products, human Sec61α1 with an additional Myc/6His tag was used (Greenfield and High, 1999). Cells were treated with *SEC61A1*-UTR or *SEC63*-UTR siRNA as described above for 96 hr. Six hours after the second transfection (*SEC61A1*-UTR siRNA) or 24 hr before harvesting (*SEC63*-UTR siRNA), the siRNA-treated cells were transfected with either vector or expression plasmid using Fugene HD (Promega). Based on GFP fluorescence, the transfection efficiency was ~80%.

Protein Transport

Precursor polypeptides were synthesized in reticulocyte lysate (nuclease treated; Promega) in the presence of [^{35}S]methionine (PerkinElmer) and buffer or semipermeabilized cells (final concentration: 3,200 to 12,800 cell equivalents/μL) for 60 min at 30°C (co-translational transport). Notably, the membrane concentration was in the linear range for the assay. Alternatively, precursor polypeptides were synthesized in reticulocyte lysate in the presence of [^{35}S]methionine for 15 min at 30°C. After 5-min incubation with puromycin (final concentration: 1 mM) at 30°C, buffer or semipermeabilized cells (final concentration: 12,800 cell equivalents/μL) were added and the incubation continued for 20 min (post-translational transport). The cells were pre-treated with targeting or control siRNA for 96 hr and transfected with expression or control vector where indicated. Semipermeabilized cells were prepared from equal cell numbers by digitonin treatment according to the published procedure (Johnson et al., 2012; Lang et al., 2012). The concentration was adjusted according to optical density at 280 nm (OD_{280}) in 2% SDS and eventually confirmed by SDS-PAGE and protein staining. Following translocation, membranes were re-isolated by centrifugation at 125,000 × *g* at 4°C for 20 min when required. Where indicated, sequestration assays were performed for 60 min at 0°C in 80 mM sucrose supplemented with combinations of proteinase K (20 μg/mL) and Triton X-100 (2%) or H_2O as indicated. Proteolysis was stopped by the addition of PMSF (final concentration: 20 mM) and incubation continued for 5 min at 0°C. All samples were analyzed by SDS-PAGE and phosphorimaging (Typhoon-Trio imaging system). Image Quant TL 7.0 was used for quantifications. Silencing efficiency was evaluated by western blot.

Alternatively, programmed reticulocyte lysate was supplemented with canine pancreatic rough microsomes and CAM741 (final concentration: 25 μM) or DMSO. After incubation for 30 min at 0°C, co-translational protein translocation in the presence of [^{35}S]methionine (PerkinElmer) was initiated by shifting the temperature to 30°C for 60 min. For post-translational translocation, protein synthesis was carried out for 15 min at 30°C in the presence of [^{35}S]methionine before supplementing with rough microsomes and CAM741 or DMSO, respectively. Similarly, after incubation for 30 min at 0°C, post-translational protein translocation was initiated by shifting the temperature to 30°C for 20 min.

Chemical Crosslinking

BMH was used for crosslinking. Following translocation, membranes were sedimented by centrifugation (125,000 × *g* for 20 min at 4°C). The pellet was resuspended in XL-buffer (50 mM HEPES-KOH [pH 7.5], 50 mM K-acetate, 2 mM Mg-acetate, and 200 mM sucrose) and supplemented with BMH (final concentration: 2.5 mM) or DMSO. Crosslinking was carried out for 30 min at room temperature and terminated by the addition of SDS sample buffer or adjustment to 20 mM β-mercaptoethanol. Where indicated, immunoprecipitation with validated antibodies was carried out after membrane solubilization in 0.65% 3-[(3-cholamidopropyl)dimethylammonio]-1-propanesulfonate (CHAPS) and 0.4 M KCl as described (Tyedmers et al., 2000). Alternatively, membranes were solubilized in 1% SDS and 10 mM TRIS-HCl (pH 7.5), and immunoprecipitation was carried out at final concentrations of 0.1% SDS, 1% Triton X-100, 140 mM NaCl, 1 mM EDTA, and 10 mM TRIS-HCl (pH 7.5) (Abell et al., 2003).

Graphical Representation and Statistical Analysis

Dot plots depict relative targeting efficiencies calculated as the proportion of N-glycosylation and/or signal peptide cleavage of the total amount of synthesized precursors with the individual control sample set to 100%. Data points and the mean of at least three independent experiments were visualized with GraphPad Prism 5 software. For statistical comparison between a treatment group and the corresponding control, a Student's t test was used (indicated by the upper panel). To compare between multiple precursor variants or treatment groups (indicated by horizontal brackets), ANOVA was performed, including the post hoc Dunnett's or Newman-Keuls test, respectively, using normalized values. Significance levels are given as follows: $p < 0.001$ (***); $p < 0.01$ (**); and $p < 0.05$ (*).

SUPPLEMENTAL INFORMATION

Supplemental Information includes seven figures and three tables and can be found with this article online at https://doi.org/10.1016/j.celrep.2018.03.122.

ACKNOWLEDGMENTS

We are thankful to S. Fedeles and S. Somlo (New Haven, USA) for Sec63-null cells, to Novartis (Basel Switzerland) for CAM741, to M.-C. Klein (Homburg) for the *SEC61A1*Myc/*6His* plasmid, and to N. Aviram (Rehovot, Israel) for helpful comments on the manuscript. This work was supported by a Wellcome Trust Investigator Award in Science (204957/Z/16/Z) and by grants from the Deutsche Forschungsgemeinschaft (IRTG 1830 and ZI 234/13-1).

AUTHOR CONTRIBUTIONS

Conceptualization, S. Haßdenteufel and R.Z.; Methodology, A.W.P., J.C.P., N.J., and S. High; Investigation, S. Haßdenteufel; Resources, A.W.P., J.C.P., N.J., and S. High; Writing – Original Draft, S. Haßdenteufel and R.Z.; Writing – Review & Editing, S. Haßdenteufel, N.J., S. High, and R.Z.; Visualization, S. Haßdenteufel; Project Administration, R.Z.; Funding Acquisition, S. High and R.Z.

DECLARATION OF INTERESTS

The authors declare no competing interests.

Received: September 5, 2017
Revised: February 15, 2018
Accepted: March 27, 2018
Published: May 1, 2018

REFERENCES

Abell, B.M., Jung, M., Oliver, J.D., Knight, B.C., Tyedmers, J., Zimmermann, R., and High, S. (2003). Tail-anchored and signal-anchored proteins utilize overlapping pathways during membrane insertion. J. Biol. Chem. *278*, 5669–5678.

Aviram, N., and Schuldiner, M. (2014). Embracing the void–how much do we really know about targeting and translocation to the endoplasmic reticulum? Curr. Opin. Cell Biol. *29*, 8–17.

Aviram, N., Ast, T., Costa, E.A., Arakel, E.C., Chuartzman, S.G., Jan, C.H., Haßdenteufel, S., Dudek, J., Jung, M., Schorr, S., et al. (2016). The SND proteins constitute an alternative targeting route to the endoplasmic reticulum. Nature *540*, 134–138.

Conti, B.J., Devaraneni, P.K., Yang, Z., David, L.L., and Skach, W.R. (2015). Cotranslational stabilization of Sec62/63 within the ER Sec61 translocon is controlled by distinct substrate-driven translocation events. Mol. Cell *58*, 269–283.

Davis, E.M., Kim, J., Menasche, B.L., Sheppard, J., Liu, X., Tan, A.-C., and Shen, J. (2015). Comparative haploid genetic screens reveal divergent pathways in the biogenesis and trafficking of glycophosphatidylinositol-anchored proteins. Cell Rep. *11*, 1727–1736.

Dejgaard, K., Theberge, J.-F., Heath-Engel, H., Chevet, E., Tremblay, M.L., and Thomas, D.Y. (2010). Organization of the Sec61 translocon, studied by high resolution native electrophoresis. J. Proteome Res. *9*, 1763–1771.

Dudek, J., Pfeffer, S., Lee, P.-H., Jung, M., Cavalié, A., Helms, V., Förster, F., and Zimmermann, R. (2015). Protein transport into the human endoplasmic reticulum. J. Mol. Biol. *427* (*6 Pt A*), 1159–1175.

Fedeles, S.V., Tian, X., Gallagher, A.-R., Mitobe, M., Nishio, S., Lee, S.H., Cai, Y., Geng, L., Crews, C.M., and Somlo, S. (2011). A genetic interaction network of five genes for human polycystic kidney and liver diseases defines polycystin-1 as the central determinant of cyst formation. Nat. Genet. *43*, 639–647.

Görlich, D., and Rapoport, T.A. (1993). Protein translocation into proteoliposomes reconstituted from purified components of the endoplasmic reticulum membrane. Cell *75*, 615–630.

Greenfield, J.J.A., and High, S. (1999). The Sec61 complex is located in both the ER and the ER-Golgi intermediate compartment. J. Cell Sci. *112*, 1477–1486.

Haßdenteufel, S., Sicking, M., Schorr, S., Aviram, N., Fecher-Trost, C., Schuldiner, M., Jung, M., Zimmermann, R., and Lang, S. (2017). hSnd2 protein represents an alternative targeting factor to the endoplasmic reticulum in human cells. FEBS Lett. *591*, 3211–3224.

Hegde, R.S., and Bernstein, H.D. (2006). The surprising complexity of signal sequences. Trends Biochem. Sci. *31*, 563–571.

Johnson, N., Vilardi, F., Lang, S., Leznicki, P., Zimmermann, R., and High, S. (2012). TRC40 can deliver short secretory proteins to the Sec61 translocon. J. Cell Sci. *125*, 3612–3620.

Johnson, N., Haßdenteufel, S., Theis, M., Paton, A.W., Paton, J.C., Zimmermann, R., and High, S. (2013). The signal sequence influences post-translational ER translocation at distinct stages. PLoS ONE *8*, e75394.

Lakkaraju, A.K.K., Thankappan, R., Mary, C., Garrison, J.L., Taunton, J., and Strub, K. (2012). Efficient secretion of small proteins in mammalian cells relies on Sec62-dependent posttranslational translocation. Mol. Biol. Cell *23*, 2712–2722.

Lang, S., Benedix, J., Fedeles, S.V., Schorr, S., Schirra, C., Schäuble, N., Jalal, C., Greiner, M., Hassdenteufel, S., Tatzelt, J., et al. (2012). Different effects of Sec61α, Sec62 and Sec63 depletion on transport of polypeptides into the endoplasmic reticulum of mammalian cells. J. Cell Sci. *125*, 1958–1969.

Lloyd, D.J., Wheeler, M.C., and Gekakis, N. (2010). A point mutation in Sec61α1 leads to diabetes and hepatosteatosis in mice. Diabetes *59*, 460–470.

Mackinnon, A.L., Paavilainen, V.O., Sharma, A., Hegde, R.S., and Taunton, J. (2014). An allosteric Sec61 inhibitor traps nascent transmembrane helices at the lateral gate. eLife *3*, e01483.

Müller, G., and Zimmermann, R. (1987). Import of honeybee prepromelittin into the endoplasmic reticulum: structural basis for independence of SRP and docking protein. EMBO J. *6*, 2099–2107.

Müller, G., and Zimmermann, R. (1988). Import of honeybee prepromelittin into the endoplasmic reticulum: energy requirements for membrane insertion. EMBO J. *7*, 639–648.

Müller, L., de Escauriaza, M.D., Lajoie, P., Theis, M., Jung, M., Müller, A., Burgard, C., Greiner, M., Snapp, E.L., Dudek, J., and Zimmermann, R. (2010). Evolutionary gain of function for the ER membrane protein Sec62 from yeast to humans. Mol. Biol. Cell *21*, 691–703.

Nilsson, I., Lara, P., Hessa, T., Johnson, A.E., von Heijne, G., and Karamyshev, A.L. (2015). The code for directing proteins for translocation across ER membrane: SRP cotranslationally recognizes specific features of a signal sequence. J. Mol. Biol. *427* (*6 Pt A*), 1191–1201.

Paton, A.W., Beddoe, T., Thorpe, C.M., Whisstock, J.C., Wilce, M.C., Rossjohn, J., Talbot, U.M., and Paton, J.C. (2006). AB5 subtilase cytotoxin inactivates the endoplasmic reticulum chaperone BiP. Nature *443*, 548–552.

Reithinger, J.H., Kim, J.E.H., and Kim, H. (2013). Sec62 protein mediates membrane insertion and orientation of moderately hydrophobic signal anchor proteins in the endoplasmic reticulum (ER). J. Biol. Chem. *288*, 18058–18067.

Schäuble, N., Lang, S., Jung, M., Cappel, S., Schorr, S., Ulucan, Ö., Linxweiler, J., Dudek, J., Blum, R., Helms, V., et al. (2012). BiP-mediated closing of the Sec61 channel limits Ca^{2+} leakage from the ER. EMBO J. *31*, 3282–3296.

Schlenstedt, G., and Zimmermann, R. (1987). Import of frog prepropeptide GLa into microsomes requires ATP but does not involve docking protein or ribosomes. EMBO J. *6*, 699–703.

Schlenstedt, G., Gudmundsson, G.H., Boman, H.G., and Zimmermann, R. (1990). A large presecretory protein translocates both cotranslationally, using signal recognition particle and ribosome, and post-translationally, without these ribonucleoparticles, when synthesized in the presence of mammalian microsomes. J. Biol. Chem. *265*, 13960–13968.

Shao, S., and Hegde, R.S. (2011). A calmodulin-dependent translocation pathway for small secretory proteins. Cell *147*, 1576–1588.

Shin, K., Pandey, A., Liu, X.Q., Anini, Y., and Rainey, J.K. (2013). Preferential apelin-13 production by the proprotein convertase PCSK3 is implicated in obesity. FEBS Open Bio *3*, 328–333.

Tyedmers, J., Lerner, M., Bies, C., Dudek, J., Skowronek, M.H., Haas, I.G., Heim, N., Nastainczyk, W., Volkmer, J., and Zimmermann, R. (2000). Homologs of the yeast Sec complex subunits Sec62p and Sec63p are abundant proteins in dog pancreas microsomes. Proc. Natl. Acad. Sci. USA *97*, 7214–7219.

von Heijne, G. (1985). Signal sequences. The limits of variation. J. Mol. Biol. *184*, 99–105.

Voorhees, R.M., and Hegde, R.S. (2016). Structure of the Sec61 channel opened by a signal sequence. Science *351*, 88–91.

Wirth, A., Jung, M., Bies, C., Frien, M., Tyedmers, J., Zimmermann, R., and Wagner, R. (2003). The Sec61p complex is a dynamic precursor activated channel. Mol. Cell *12*, 261–268.

Yanagitani, K., Kimata, Y., Kadokura, H., and Kohno, K. (2011). Translational pausing ensures membrane targeting and cytoplasmic splicing of XBP1u mRNA. Science *331*, 586–589.

Zhang, B., and Miller, T.F., 3rd. (2012). Long-timescale dynamics and regulation of Sec-facilitated protein translocation. Cell Rep. *2*, 927–937.

Cell Reports, Volume *23*

Supplemental Information

Chaperone-Mediated Sec61 Channel Gating during ER Import of Small Precursor Proteins Overcomes Sec61 Inhibitor-Reinforced Energy Barrier

Sarah Haßdenteufel, Nicholas Johnson, Adrienne W. Paton, James C. Paton, Stephen High, and Richard Zimmermann

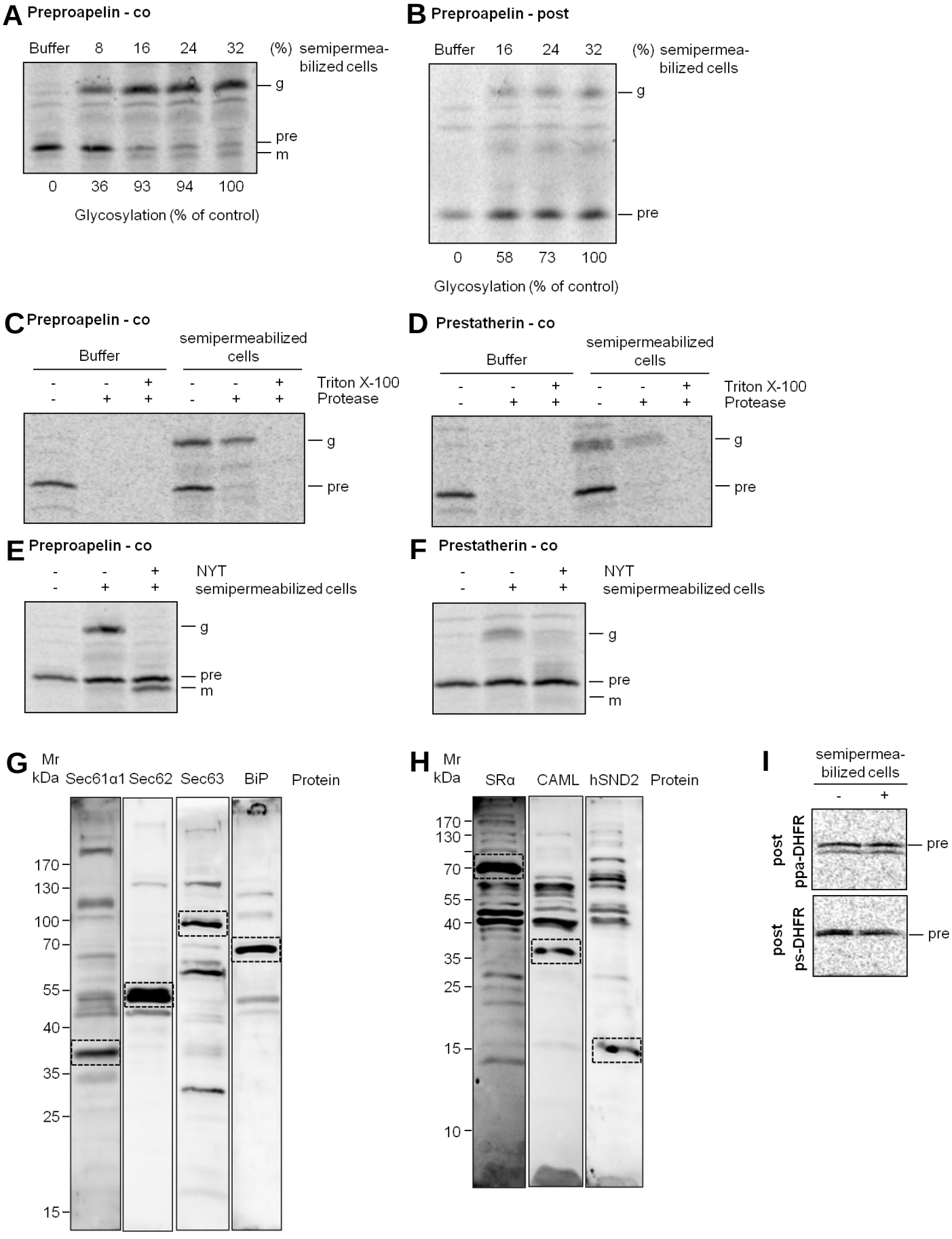
A
Preproapelin - co
Buffer 8 16 24 32 (%) semipermeabilized cells
g
pre
m
0 36 93 94 100
Glycosylation (% of control)
B
Preproapelin - post
Buffer 16 24 32 (%) semipermeabilized cells
g
pre
0 58 73 100
Glycosylation (% of control)
C
Preproapelin - co
Buffer
semipermeabilized cells
Triton X-100
Protease
g
pre
D
Prestatherin - co
Buffer
semipermeabilized cells
Triton X-100
Protease
g
pre
E
Preproapelin - co
NYT
semipermeabilized cells
g
pre
m
F
Prestatherin - co
NYT
semipermeabilized cells
g
pre
m
G
Mr kDa
Sec61α1 Sec62 Sec63 BiP Protein
170
130
100
70
55
40
35
25
15
H
Mr kDa
SRα CAML hSND2 Protein
170
130
70
55
40
35
25
15
10
I
semipermeabilized cells
post ppa-DHFR
pre
post ps-DHFR
pre

Figure S1. Transport of preproapelin and prestatherin into the human ER, Related to Figure 1.

Note that under co-translational conditions, precursor polypeptide chains and fully-synthesized precursors were targeted and inserted into Sec61 complexes. Under post-translational conditions, only the targeting and membrane insertion of completed precursor polypeptides occurred. **A-B)** Titration of HeLa cell-derived ER membranes in ppa translocation defined the linear range of the assay. Following semipermeabilization of untreated HeLa cells, ppa was co- (co, **A**) or post-translationally (post, **B**) incubated with the indicated concentrations of ER membranes (8% to 32% v/v of the total translation mix, equivalent to 3,200 to 12,800 cell equivalents/µl). **C-D)** Sequestration assay for demonstration of complete ppa and ps translocation. Following co-translational incubation of ppa **(C)** or ps **(D)** with untreated semipermeabilized HeLa cells (3,200 cell equivalents/µl), membranes were re-isolated in sucrose supplemented with combinations of proteinase K and Triton X-100 as indicated. **E-F)** Transport in the presence of the tripeptide NYT for demonstration of N-glycosylation. Following semipermeabilization of untreated HeLa cells, ppa **(E)** or ps **(F)** were co-translationally incubated with ER membranes (3,200 cell equivalents/µl) in the presence of NYT (0.5 mM). Radioactive samples were subjected to SDS-PAGE and phosphorimaging. Transport efficiencies were calculated as the proportion of N-glycosylation on the total amount of synthesized precursor with the control sample set to 100%. Shown are the relevant parts of representative phosphorimages. Pre: precursor polypeptide; m: mature protein; g: singly or doubly glycosylated protein. **G, H**) HeLa cells were characterized with validated antibodies by Western blot (Lang et al., 2012; Johnson et al., 2013; Haßdenteufel et al., 2017). Shown are representative blot images. The respective protein of interest was identified by its absence in siRNA treated cells (see Figures S2-5) and is boxed with broken lines. **I**) In contrast to Figure 1C, the indicated precursors were post-translationally incubated with the

ER membranes. Notably, there was no signal peptide cleavage in the presence of semi-permeabilized cells under these conditions.

Fig. S2

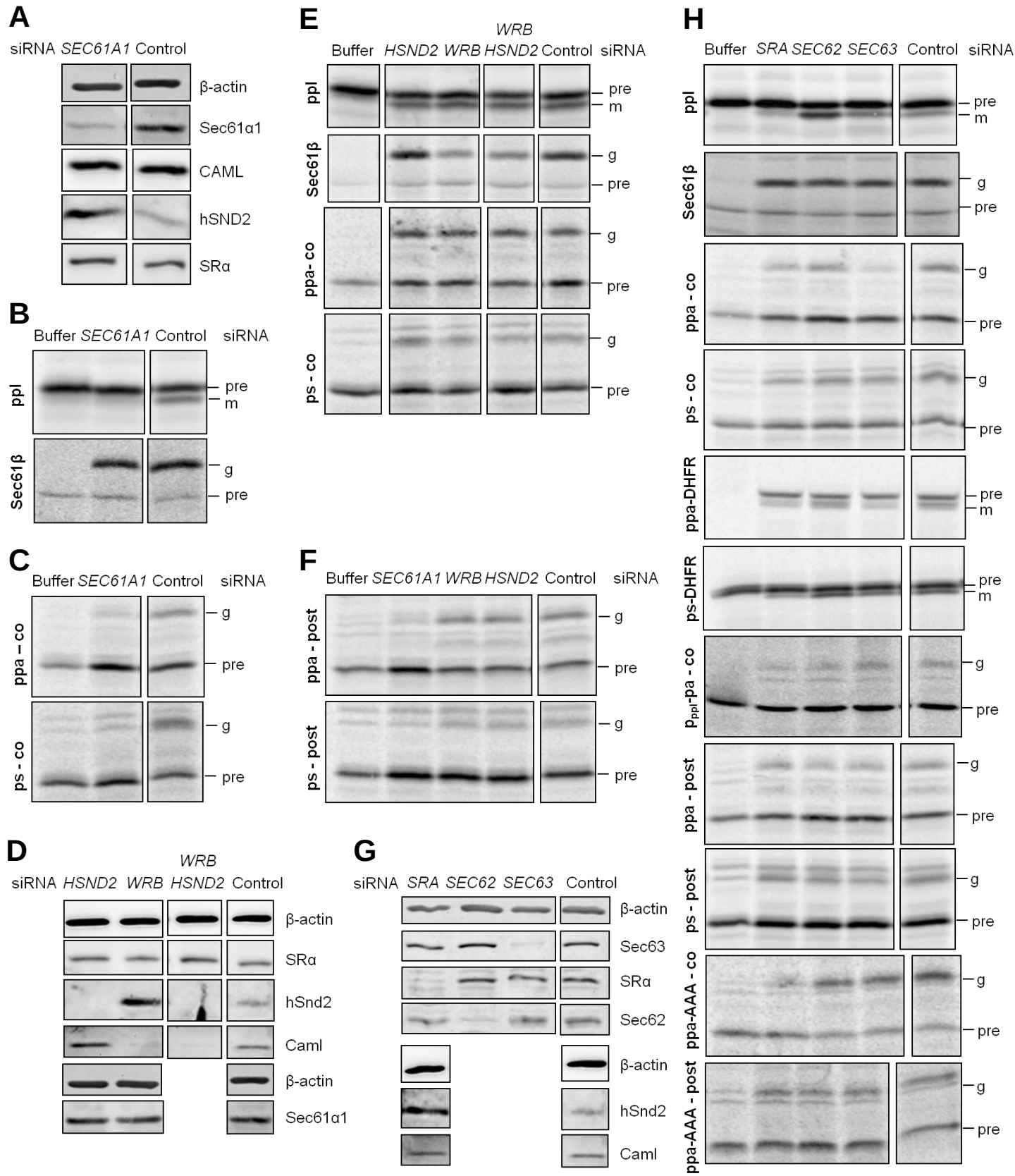
A
siRNA SEC61A1 Control
β-actin
Sec61α1
CAML
hSND2
SRα
B
Buffer SEC61A1 Control siRNA
ppl
pre
m
Sec61β
g
pre
C
Buffer SEC61A1 Control siRNA
ppa – co
g
pre
ps - co
g
pre
D
WRB
siRNA HSND2 WRB HSND2 Control
β-actin
SRα
hSnd2
Caml
β-actin
Sec61α1
E
WRB
Buffer HSND2 WRB HSND2 Control siRNA
ppl
pre
m
Sec61β
g
pre
ppa- co
g
pre
ps - co
g
pre
F
Buffer SEC61A1 WRB HSND2 Control siRNA
ppa - post
g
pre
ps - post
g
pre
G
siRNA SRA SEC62 SEC63 Control
β-actin
Sec63
SRα
Sec62
β-actin
hSnd2
Caml
H
Buffer SRA SEC62 SEC63 Control siRNA
ppl
pre
m
Sec61β
g
pre
ppa - co
g
pre
ps - co
g
pre
ppa-DHFR
pre
m
ps-DHFR
pre
m
pPpl-pa - co
g
pre
ppa - post
g
pre
ps - post
g
pre
ppa-AAA - co
g
pre
ppa-AAA - post
g
pre

Figure S2. Effects of Sec61α1, Sec62, Sec63, SRα, hSnd2 and Wrb depletion on transport of short presecretory proteins, Related to Figures 2 and 3.

A, D, G) Representative Western blots validating protein content. **B-C, E, F, H)** Phosphorimages of representative SDS-PAGE gels. Prior to preparation of semipermeabilized cells, HeLa cells were treated with the indicated siRNA(s). Precursors were co- (co) or post-translationally (post) incubated with the indicated ER membranes. Pre: precursor polypeptide; m: mature protein; g: glycosylated protein.

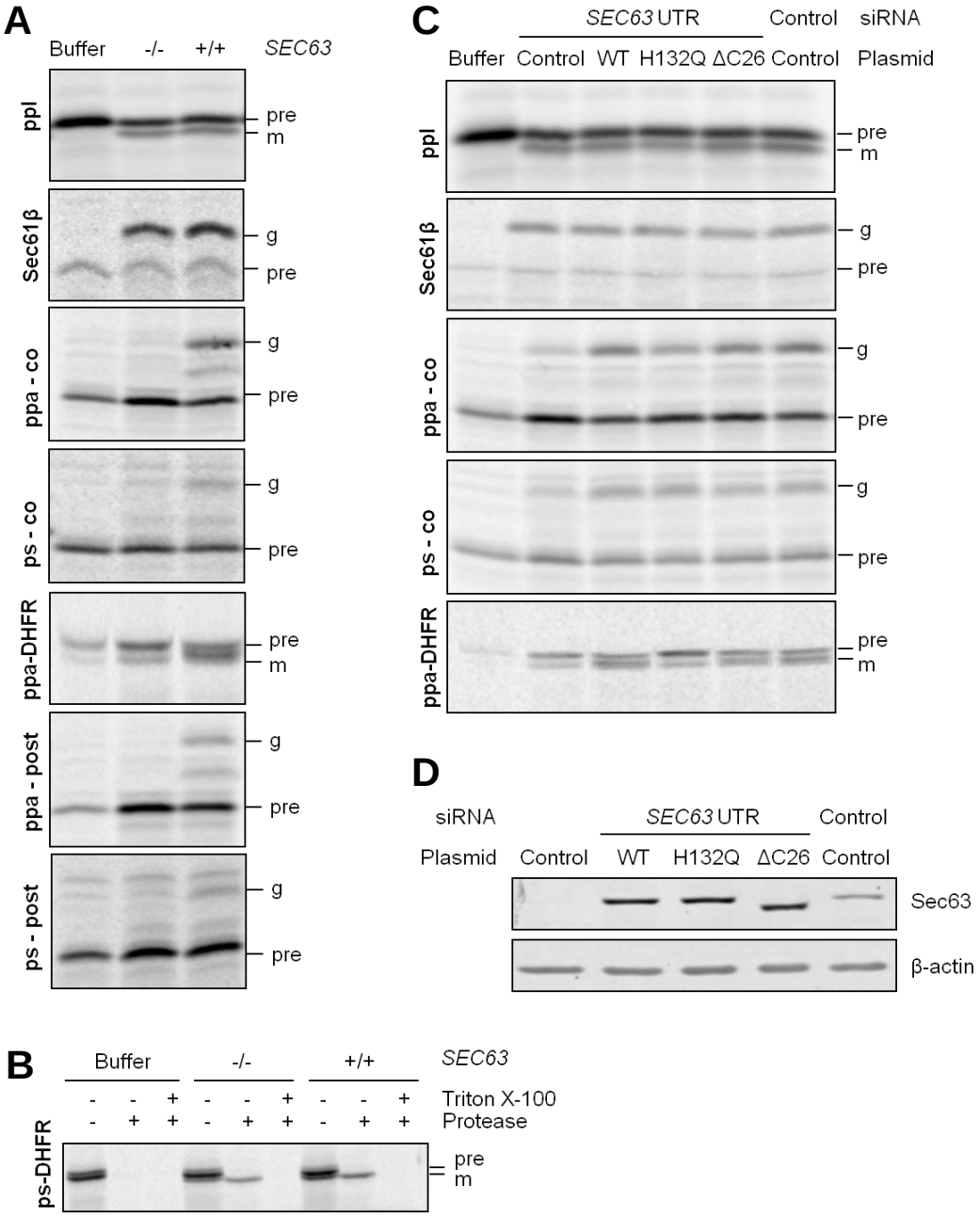
A
Buffer
-/-
+/+
SEC63
ppl
pre
m
Sec61β
g
pre
ppa - co
ps - co
ppa-DHFR
ppa - post
ps - post
C
SEC63 UTR
Control
siRNA
Buffer
Control
WT
H132Q
ΔC26
Control
Plasmid
D
siRNA
SEC63 UTR
Control
Plasmid
Control
WT
H132Q
ΔC26
Control
Sec63
β-actin
B
Buffer
-/-
+/+
SEC63
Triton X-100
Protease
ps-DHFR
pre
m

Figure S3. Effects of murine *SEC63* knock-out on transport of short presecretory proteins and complementation of *SEC63* siRNA effects, **Related to Figure 3.**

A-C) Phosphorimages of representative SDS-PAGE gels. **D)** Representative Western blot validating protein content. Semipermeabilized cells were prepared from murine *SEC63*-null cells **(A, B)** or HeLa cells **(C, D)**. Prior to preparation, HeLa cells were treated with *SEC63*-UTR siRNA and transfected with the indicated plasmids. Precursors were co- (co) or post-translationally (post) incubated with the indicated ER membranes. Pre: precursor polypeptide; m: mature protein; g: glycosylated protein.

Fig. S4

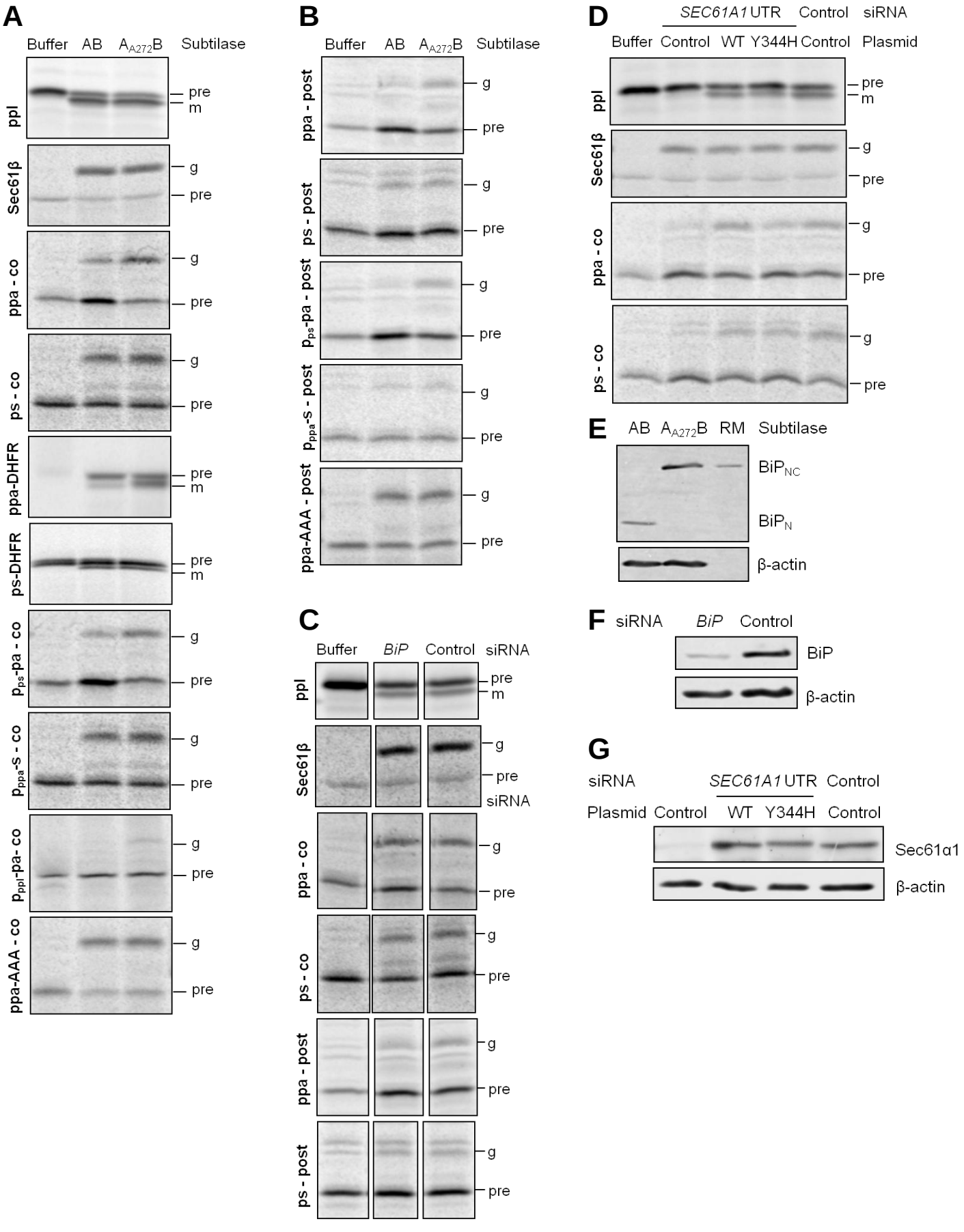
A
Buffer
AB
$A_{A272}B$
Subtilase
ppl
Sec61β
ppa - co
ps - co
ppa-DHFR
ps-DHFR
p_{ps}-pa - co
p_{ppa}-s - co
p_{ppl}-pa- co
ppa-AAA - co
pre
m
g
B
ppa - post
ps - post
p_{ps}-pa - post
p_{ppa}-s - post
ppa-AAA - post
C
Buffer
BiP
Control
siRNA
D
SEC61A1 UTR
Control
siRNA
Buffer
Control
WT
Y344H
Control
Plasmid
E
AB
$A_{A272}B$
RM
Subtilase
BiP_{NC}
BiP_N
β-actin
F
siRNA
BiP
Control
BiP
β-actin
G
siRNA
SEC61A1 UTR
Control
Plasmid
Control
WT
Y344H
Control
Sec61α1
β-actin

Figure S4. Effects of of subtilase toxin and *BIP* siRNA on transport of short presecretory proteins and complementation of *SEC61A1* siRNA effects, Related to Figure 4.

A-D) Phosphorimages of representative SDS-PAGE gels. **E-G)** Representative Western blots validating protein content. Prior to preparation of semipermeabilized cells, HeLa cells were treated with active or inactive subtilase toxin (**A, B, E**), with *BIP* **(C, F)** or *SEC61A1*-UTR siRNA and transfected with the indicated plasmids (**D, G)**. Precursors were co- (co) or post-translationally (post) incubated with the indicated ER membranes. Pre: precursor polypeptide; m: mature protein; g: glycosylated protein.

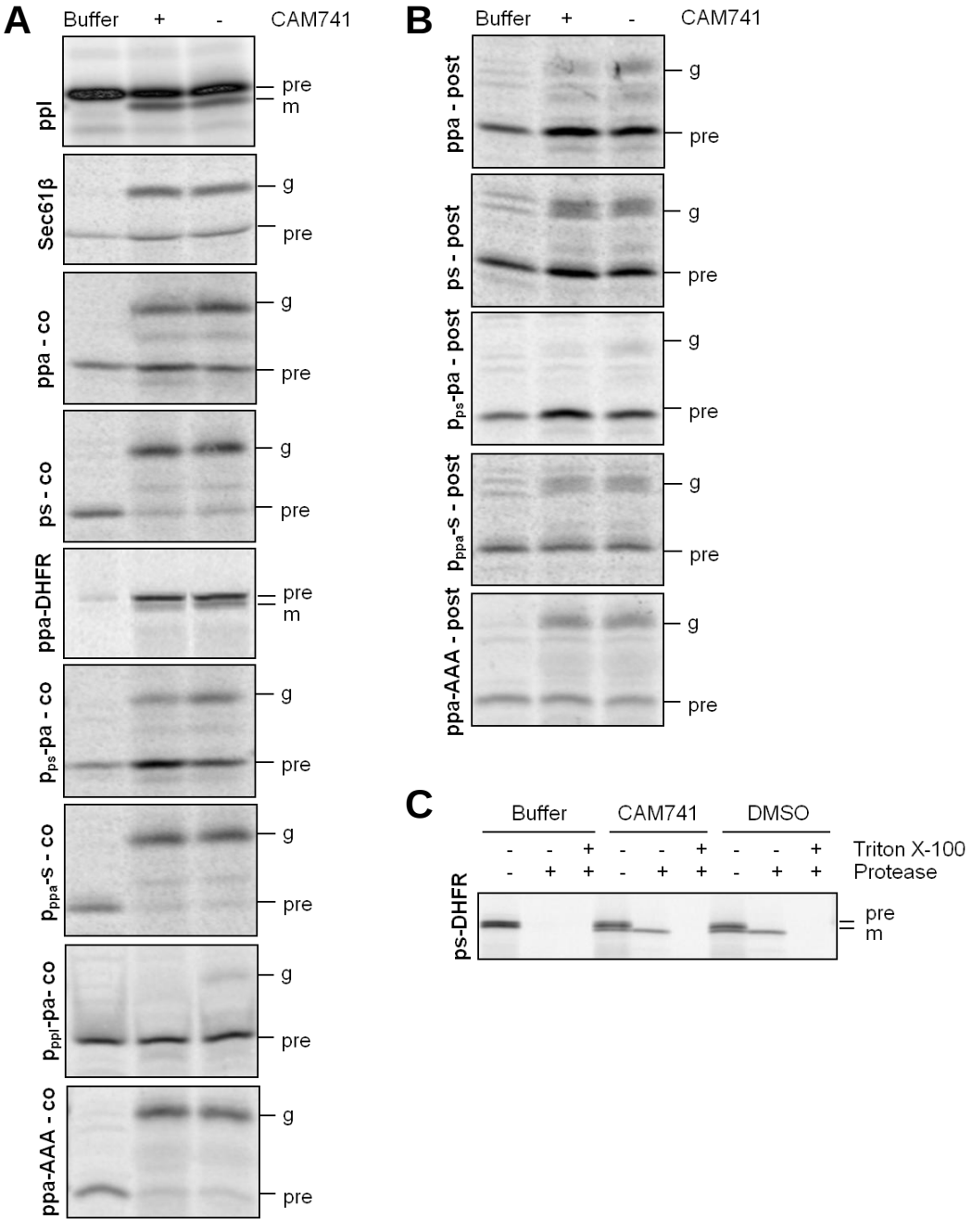
A
Buffer
+
-
CAM741
ppl
pre
m
Sec61β
g
pre
ppa - co
g
pre
ps - co
g
pre
ppa-DHFR
pre
m
p_{ps}-pa - co
g
pre
p_{ppa}-s - co
g
pre
p_{ppl}-pa- co
g
pre
ppa-AAA - co
g
pre
B
Buffer
+
-
CAM741
ppa - post
g
pre
ps - post
g
pre
p_{ps}-pa - post
g
pre
p_{ppa}-s - post
g
pre
ppa-AAA - post
g
pre
C
Buffer
CAM741
DMSO
Triton X-100
Protease
ps-DHFR
pre
m

Figure S5. Effects of CAM741 on transport of short presecretory proteins, Related to Figure 5.

A-C) Phosphorimages of representative SDS-PAGE gels. Precursors were co- (co) or post-translationally (post) incubated with canine pancreatic rough microsomes in the presence of solvent or CAM741. Pre: precursor polypeptide; m: mature protein; g: glycosylated protein.

Fig. S6

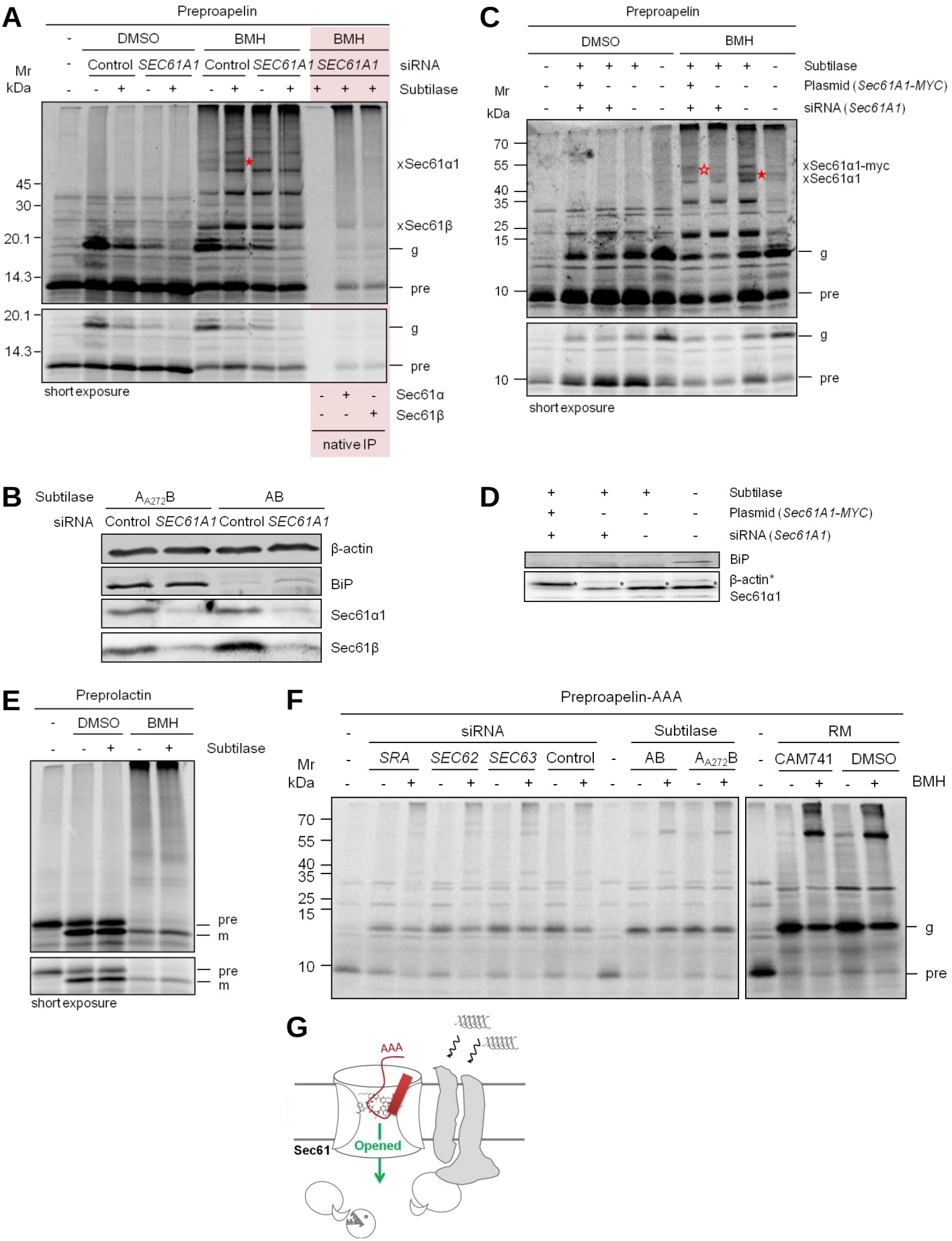
A
Preproapelin
DMSO
BMH
BMH
Mr
kDa
Control
SEC61A1
Control
SEC61A1
SEC61A1
siRNA
Subtilase
45
30
20.1
14.3
xSec61α1
xSec61β
g
pre
20.1
14.3
g
pre
short exposure
Sec61α
Sec61β
native IP
C
Preproapelin
DMSO
BMH
Subtilase
Plasmid (Sec61A1-MYC)
siRNA (Sec61A1)
Mr
kDa
70
55
40
35
25
15
10
xSec61α1-myc
xSec61α1
g
pre
10
g
pre
short exposure
B
Subtilase
A272B
AB
siRNA
Control
SEC61A1
Control
SEC61A1
β-actin
BiP
Sec61α1
Sec61β
D
Subtilase
Plasmid (Sec61A1-MYC)
siRNA (Sec61A1)
BiP
β-actin*
Sec61α1
E
Preprolactin
DMSO
BMH
Subtilase
pre
m
pre
m
short exposure
F
Preproapelin-AAA
siRNA
Subtilase
RM
Mr
kDa
SRA
SEC62
SEC63
Control
AB
A272B
CAM741
DMSO
BMH
70
55
40
35
25
15
10
g
pre
G
AAA
Sec61
Opened

Figure S6. Identification of Sec61α1 and Sec61β as crosslinking partners of preproapelin upon co-translational translocation in the absence of BiP or Sec61 complex and crosslinking of ppl and preproapelin-AAA, Related to Figure 6.

A-D) Identification of crosslinking partners of ppa in the absence of Sec61 complex (**A, B**) or BiP (**A-D**) and in the presence of tagged Sec61α, respectively (**C, D**). HeLa cells were treated with *SEC61A1*-UTR siRNA or control siRNA and transfected with *SEC61A1*-Myc/6His or control plasmid, and then treated with subtilase AB or inactive subtilase variant $A_{A272}B$. Following the preparation of semipermeabilized cells used for co-translational translocation of ppa, membranes were obtained by sedimentation, re-suspended in XL-buffer, and supplemented with BMH or DMSO for crosslinking. Radioactive samples were subjected to SDS-PAGE and phosphorimaging. Where indicated, immunoprecipitation with validated antibodies was carried out after crosslinking and membrane solubilisation under non-denaturing conditions (0.65% CHAPS and 0.4 M KCl; Tyedmers et al., 2000; **A**). Relevant crosslinking products of ppa to Sec61α1 (filled red asterisk), Sec61α1-Myc/6His (open red asterisk) or Sec61β (blue asterisk) are indicated. Pre: precursor polypeptide; g, glycosylated protein. **B, D)** Protein content was validated by Western blot. We note that the tagged Sec61α comigrated with ß-actin (**D**). **E, F)** Crosslinking of fully-synthesized ppl (**E**) and ppa-AAA (**F**). Prior to preparation of semipermeabilized cells, HeLa cells were treated with the indicated siRNA (Table 1) or subtilase toxin. Alternatively, canine pancreatic rough microsomes were treated with solvent or CAM741. The presecretory proteins ppl and ppa-AAA were co-translationally incubated with the indicated ER membranes, which were sedimented and re-suspended in XL-buffer before crosslinking with BMH. Radioactively labelled samples were subjected to SDS-PAGE and phosphorimaging. pre: precursor polypeptide; g: glycosylated protein; m, mature protein. **G)** Schematic representation of

ppa-AAA translocation upon depletion of Sec62, Sec63 or BiP by siRNA (waved arrows) or toxin (pacman) treatment, or in the presence of CAM741. Without the help by accessory translocon components, insertion into the Sec61-channel efficiently occurs without trapping of ppa-AAA precursor polypeptides.

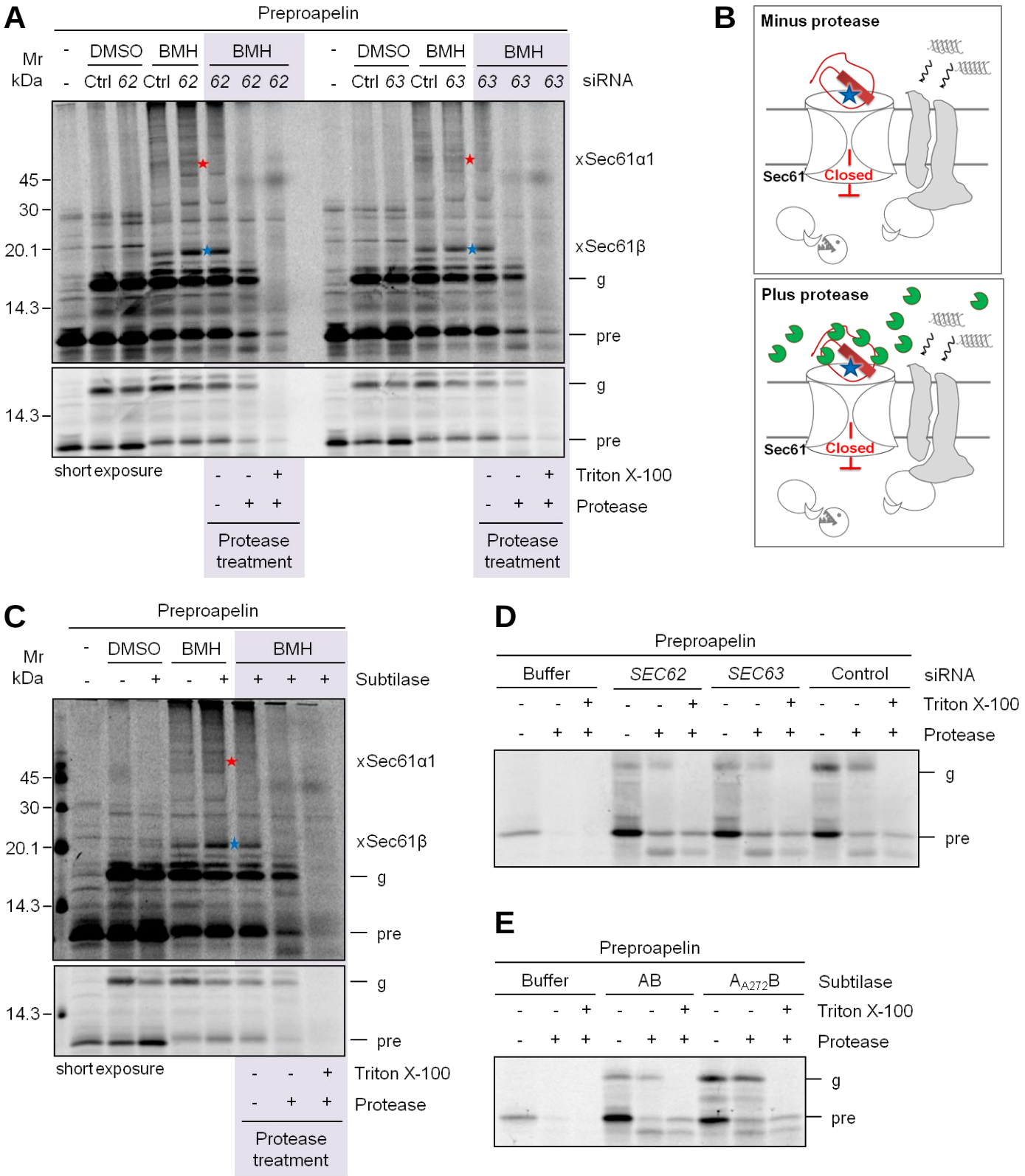
A
Preproapelin
Mr
kDa
- DMSO BMH BMH
- Ctrl 62 Ctrl 62 62 62 62
- DMSO BMH BMH
- Ctrl 63 Ctrl 63 63 63 63
siRNA
45
30
20.1
14.3
xSec61α1
xSec61β
g
pre
14.3
g
pre
short exposure
- - + Triton X-100
- + + Protease
Protease treatment
B
Minus protease
Sec61
Closed
Plus protease
Sec61
Closed
C
Preproapelin
Mr
kDa
- DMSO BMH BMH
- - + - + + + + Subtilase
45
30
20.1
14.3
xSec61α1
xSec61β
g
pre
14.3
g
pre
short exposure
- - + Triton X-100
- + + Protease
Protease treatment
D
Preproapelin
Buffer SEC62 SEC63 Control siRNA
- - + - - + - - + - - + Triton X-100
- + + - + + - + + - + + Protease
g
pre
E
Preproapelin
Buffer AB A272B Subtilase
- - + - - + - - + Triton X-100
- + + - + + - + + Protease
g
pre

Figure S7. Localisation of preproapelin and its crosslinking products after co-translational translocation in the absence of Sec62, Sec63, or BiP, Related to Figure 6.

A-E) Prior to preparation of semipermeabilized cells, HeLa cells were treated with the indicated siRNA or subtilase cytotoxin. ppa was co-translationally incubated with the indicated ER membranes, which were sedimented and resuspended in XL-buffer before sequestration analysis (i.e., treatment with proteinase K (green pacman in **B**) in the absence or presence of Triton X-100) and/or crosslinking with BMH plus subsequent sequestration analysis. Samples were subjected to SDS-PAGE and phosphorimaging. Relevant crosslinking products of ppa to Sec61α1 or Sec61β are indicated by red and blue asterisks, resepctively. Pre: ppa; g: glycosylated pa. **B**) Schematic representation of ppa translocation upon depletion of Sec62, Sec63 or BiP by siRNA (waved arrows) or toxin (pacman) treatment.

Table S1. Amino acid sequences of the model proteins, Related to Figure 1.

Underlined: SP or TMD; italics: linker dipeptide; red: mutagenized positively charged cluster; blue: putative translational pausing element.

Name	Sequence
ppa OPG2	MNLRLCVQALLLLWLSLTAVCG GSLMPLPDGNGLEDGNVRHLVQPRGSRNGPGPWQGGRRKFRRQRPRLSHKGPMPF MNGTEGPNFYVPFSNKTG
p_{ppl}-pa OPG2	MDSKGSSQKGSRLLLLLVVSNLLLCQGVVS GSLMPLPDGNGLEDGNVRHLVQPRGSRNGPGPWQGGRRKFRRQRPRLSHKGPMPF MNGTEGPNFYVPFSNKTG
p_{ps}-pa OPG2	MKFLVFAFILALMVSMIGA GSLMPLPDGNGLEDGNVRHLVQPRGSRNGPGPWQGGRRKFRRQRPRLSHKGPMPF MNGTEGPNFYVPFSNKTG
ppa-AAA OPG2	MNLRLCVQALLLLWLSLTAVCG GSLMPLPDGNGLEDGNVRHLVQPRGSRNGPGPWCGGAAAFRRQRPRLSHKGPMPF MNGTEGPNFYVPFSNKTG
ps OPG2	MKFLVFAFILALMVSMIGA DSSEEKFLRRIGRFGYGYGPYQPVPEQPLYPQPYQPQYQQYTF*MM* MNGTEGPNFYVPFSNKTG
p_{ppa}-s OPG2	MNLRLCVQALLLLWLSLTA DSSEEKFLRRIGRFGYGYGPYQPVPEQPLYPQPYQPQYQQYTF*MM* MNGTEGPNFYVPFSNKTG
ppl	MDSKGSSQKGSRLLLLLVVSNLLLCQGVVS TPVCPNGPGNCQVSLRDLFDRAVMVSHYIHDLSSEMFNEFDKRYAQGKGFITMALN SCHTSSLPTPEDKEQAQQTHHEVLMSLILGLLRSWNDPLYHLVTEVRGMKGAPDAIL SRAIEIEEENKRLLEGMEMIFGQVIPGAKETEPYPVWSGLPSLQTKDEDARYSAFYNL LHCLRRDSSKIDTYLKLLNCRIIYNNNC
Sec61β OPG1	MPAPASSTSVGSGSRSPSKLSAPRSAGSGGGSTLKQRKTTTSTTAARSRAPGGAGTGG MW RFYTDDSPGIKVGPVPVLVMSLLFIASVFMLHIWGKYNRS GPNFYVPFSNKTG
DHFR	MVRPLNCIVAVSQNMGIGKNGDLPWPPLRNEFKYFQRMTTTSSVEGKQNLVIMGRK TWFSIPEKNRPLKDRINIVLSRELKEPPRGAHFLAKSLDDALRLIEQPELASKVDMVWI VGGSSVYQEAMNQPGHLRLFVTRIMQEFESDTFFPEIDLGKYKLLPEYPGVLSEVQEE KGIKYKFEVYEKKD

Table S2. Characteristics of the model precursor proteins, Related to Figure 1.

SP: signal peptide; TMD: transmembrane domain; total: precursor excluding OPG1/2 tag; tagged: precursor including OPG1/2 tag; ΔG^{pred}: ΔG prediction; $N\text{-}in^{pred}$: N-in prediction.

Precursor variant	**Length (amino acids)** (SP/total/tagged)	**Charges** (SP)	**ΔG^{pred}** (SP or TMD)	**$N\text{-}in^{pred}$** (total/tagged)
ppa	22/77/95	1+	-0.19	0.94/0.88
ppa-DHFR	22/266/-	1+	-0.19	0.70/-
p_{ps}-pa	19/74/92	1+	-0.91	0.96/0.92
p_{ppl}-pa	30/85/103	3+1-	5.36	0.66/0.98
ppa-AAA	22/77/95	1+	-0.19	0.93/0.88
ps	19/62/82	1+	-0.91	0.36/0.33
ps-DHFR	19/251/-	1+	-0.91	0.31/-
p_{ppa}-s	22/65/85	1+	-0.19	0.32/0.26
ppl	30/229/-	3+1-	5.36	0.66/-
Sec61β	-/96/109	-	0.51	0.06/0.16

Table S3. Sequences of siRNAs used in this study, Related to Experimental Procedures.

Name	Target sequence	Source	Concentration (nM)	Time (h)
BIP siRNA	AAGCGGCTGTTTACTGCTTTT	Qiagen	30	48
SEC61A1-UTR siRNA	AACACTGAAATGTCTACGTTT	Applied	20	96
SEC61B-UTR siRNA	ACCCAACATTTCTTGGACCAA	Qiagen	20	96
SEC62 siRNA	AAGGCTGTGGCCAAGTATCTT	Applied	20	96
SEC63-UTR siRNA	AAGGGAGGTGTAGTTTTTTTA	Applied	20	96
HSND2 siRNA #2	CACCTTAAGGATGTGATCCTA	Qiagen	20	96
SRA-UTR siRNA	CACCAGAGCTTTGCTAATAAT	Qiagen	15	96
WRB siRNA	TGACACGTATGTACTAGTGAA	Qiagen	20	96